In addition, Mechanism 3 appears to be compatible with Model c (Fig. 6A), in which pro- and anti-BMP functions of Tsg can co-exist. In this interpretation, which combines Model c and Mechanism 3, Cv2 preferentially enhances the pro-BMP activity of Tsg; this activity is expected to depend heavily on the Cv2-mediated local high concentration of reservoir complexes that potentially release BMP. In contrast, the inactivation of BMPs by their entrapment in the Chordin–Tsg complex (anti-BMP) is Cv2-independent presumably because the entrapment process itself does not require the specific localization of the complexes. By using an embryonic kidney cell line, in which the pro-BMP function of Tsg is predominantly observed (Fig. 6E), we presented the practical feasibility of Model c (Fig. 6A), at least with respect to the cooperative pro-BMP function of Cv2 and Tsg. Consistent with Model c and also Mechanism 3, Cv2 exerts pro-BMP function in the presence of Tsg in this cell culture system. In the future investigations, other models must also be ruled out, including one in which Cv2 acts as an inhibitor of Tsg's anti-BMP activity, rather than as a co-factor of its pro-BMP activity (a sort of fusion of Models b and c).

This report mainly focused on the pro-BMP role of Cv2. Genetic analyses of *Bmp7;Cv2* mutants provide firm evidences that Cv2 acts predominantly as a pro-BMP factor in early nephrogenesis. In addition, a genetic enhancement in the nephron number was observed between *Cv2* and *Smad1* (Supplementary Fig. S9), indicating that Cv2 works cooperatively not only with the extracellular BMP ligand (BMP7) but also with the major transducer of BMP receptor signaling. Although these data do not argue the presence of a minor anti-BMP function of Cv2, it is considered the total Cv2 activity, at least on balance, is deviated toward the pro-BMP direction in the context of kidney development.

This report also focused on its genetic interactions with Tsg. Whereas it is beyond the scope of this genetics-based study, identifying the detailed molecular mechanisms underlying the pro-BMP function at the protein level is an important topic for future comprehensive study (Umulis et al., 2009). For instance, it will be intriguing to show the different kinetics of BMP release from complexes of Cv2 with Tsg versus Cv2 with Chordin, or the concentration or presentation of the ligand-bearing complexes to the receptor. It is also interesting to learn whether the role of mammalian Tsg in kidney development in fact depends on Chordin, especially given that Chordin and Chordin-related genes are expressed in the embryonic kidney (Supplementary Fig. S10). Because good antibodies for immunohistochemical studies of Tsg, Chordin and the tolloids are not available (our preliminary observations), we cannot currently examine whether Tsg–Chordin complexes are concentrated or specifically degraded near the cap condensate. Visualizing the dynamic localization, diffusion and processing of the complex proteins is a challenging but critical future task.

Our preliminary study showed that the decrease of nephron numbers in $Cv2^{-/-}$ kidneys (E14.5) was also moderately enhanced by adding a $Bmp4^{+/-}$ mutation similar to that observed with $Bmp7^{+/-}$ mutation (Supplementary Fig. S11). On the other hand, during late nephrogenesis, the $Bmp4^{+/-}$ mutation strongly enhanced the hydroureter phenotypes in the $Cv2^{-/-}$ kidneys (Supplementary Fig. S12). In this case, the formation of the ureter mesenchyme, which expresses *Bmp4* but not *Bmp7*, was strongly inhibited, suggesting that BMP4 cooperates with Cv2 independently of BMP7, at least in this context. Thus, whether BMP7 acts as a homodimer or a heterodimer with BMP4 in the Cv2 interaction is a remaining question for further investigation.

Conclusion

From our in vivo and in vitro observations, we conclude that Cv2, in concert with Tsg, shapes the signaling landscape in the complex organogenetic microenvironment of the kidney, creating locally restricted peaks in the BMP signal.

Acknowledgments

We are grateful to the staff of the Laboratory of Animal Resources and Genetic Engineering at the Center for Developmental Biology for their help with mouse husbandry, and to Drs. H. Enomoto, M. Eiraku, H. Inomata, and A. Takai for invaluable comments and discussion. BRE-luc and CIG were kindly provided by Drs. P. ten Djike and A. McMahon, respectively. *Smad1* knockout mice were a kind gift of Dr. K Hayashi through Dr. M. Saitou. MI is thankful to Ayumi Ikeya and Yu-ichi Ikeya for constant encouragement and support during this study. This work was supported in part by grants-in-aid from the Ministry of Education, Culture, Sports, Science and Technology of Japan (Y.S. and M.I.), the Kobe Cluster Project, and the Leading Project (Y.S.), and by the Special Postdoctoral Researchers Program of RIKEN (M.I.).

Appendix A. Supplementary data

Supplementary data associated with this article can be found, in the online version, at doi:10.1016/j.ydbio.2009.11.013.

References

Ambrosio, A.L., Taelman, V.F., Lee, H.X., Metzinger, C.A., Coffinier, C., De Robertis, E.M., 2008. Crossveinless-2 Is a BMP feedback inhibitor that binds Chordin/BMP to regulate Xenopus embryonic patterning. Dev. Cell 15, 248–260.

Binnerts, M.E., Wen, X., Cante-Barrett, K., Bright, J., Chen, H.T., Asundi, V., Sattari, P., Tang, T., Boyle, B., Funk, W., Rupp, F., 2004. Human Crossveinless-2 is a novel inhibitor of bone morphogenetic proteins. Biochem. Biophys. Res. Commun. 315, 272–280.

Cain, J.E., Hartwig, S., Bertram, J.F., Rosenblum, N.D., 2008. Bone morphogenetic protein signaling in the developing kidney: present and future. Differentiation 76, 831–842.

Chang, C., Holtzman, D.A., Chau, S., Chickering, T., Woolf, E.A., Holmgren, L.M., Bodorova, J., Gearing, D.P., Holmes, W.E., Brivanlou, A.H., 2001. Twisted gastrulation can function as a BMP antagonist. Nature 410, 483–487.

Coles, E., Christiansen, J., Economou, A., Bronner-Fraser, M., Wilkinson, D.G., 2004. A vertebrate crossveinless 2 homologue modulates BMP activity and neural crest cell migration. Development 131, 5309–5317.

Conley, C.A., Silburn, R., Singer, M.A., Ralston, A., Rohwer-Nutter, D., Olson, D.J., Gelbart, W., Blair, S.S., 2000. Crossveinless 2 contains cysteine-rich domains and is required for high levels of BMP-like activity during the formation of the cross veins in Drosophila. Development 127, 3947–3959.

Dudley, A.T., Robertson, E.J., 1997. Overlapping expression domains of bone morphogenetic protein family members potentially account for limited tissue defects in BMP7 deficient embryos. Dev. Dyn. 208, 349–362.

Dudley, A.T., Lyons, K.M., Robertson, E.J., 1995. A requirement for bone morphogenetic protein-7 during development of the mammalian kidney and eye. Genes Dev. 9, 2795–2807.

Glinka, A., Wu, W., Onichtchouk, D., Blumenstock, C., Niehrs, C., 1997. Head induction by simultaneous repression of Bmp and Wnt signalling in Xenopus. Nature 389, 517–519.

Godin, R.E., Takaesu, N.T., Robertson, E.J., Dudley, A.T., 1998. Regulation of BMP7 expression during kidney development. Development 125, 3473–3482.

Harada, K., Ogai, A., Takahashi, T., Kitakaze, M., Matsubara, H., Oh, H., 2008. Crossveinless-2 controls bone morphogenetic protein signaling during early cardiomyocyte differentiation in P19 cells. J. Biol. Chem. 283, 26705–26713.

Harland, R.M., 2001. Developmental biology. A twist on embryonic signalling. Nature 410, 423–424.

Hayashi, K., Kobayashi, T., Umino, T., Goitsuka, R., Matsui, Y., Kitamura, D., 2002. SMAD1 signaling is critical for initial commitment of germ cell lineage from mouse epiblast. Mech. Dev. 118, 99–109.

Hemmati-Brivanlou, A., Kelly, O.G., Melton, D.A., 1994. Follistatin, an antagonist of activin, is expressed in the Spemann organizer and displays direct neuralizing activity. Cell 77, 283–295.

Hogan, B.L., 1996. Bone morphogenetic proteins: multifunctional regulators of vertebrate development. Genes Dev. 10, 1580–1594.

Hsu, D.R., Economides, A.N., Wang, X., Eimon, P.M., Harland, R.M., 1998. The Xenopus dorsalizing factor Gremlin identifies a novel family of secreted proteins that antagonize BMP activities. Mol. Cell 1, 673–683.

Ikeya, M., Kawada, M., Kiyonari, H., Sasai, N., Nakao, K., Furuta, Y., Sasai, Y., 2006. Essential pro-Bmp roles of crossveinless 2 in mouse organogenesis. Development 133, 4463–4473.

Ikeya, M., Nosaka, T., Fukushima, K., Kawada, M., Furuta, Y., Kitamura, T., Sasai, Y., 2008. Twisted gastrulation mutation suppresses skeletal defect phenotypes in Crossveinless 2 mutant mice. Mech. Dev. 125, 832–842.

Kamimura, M., Matsumoto, K., Koshiba-Takeuchi, K., Ogura, T., 2004. Vertebrate crossveinless 2 is secreted and acts as an extracellular modulator of the BMP signaling cascade. Dev. Dyn. 230, 434–445.
Kelley, R., Ren, R., Pi, X., Wu, Y., Moreno, I., Willis, M., Moser, M., Ross, M., Podkowa, M., Attisano, L., Patterson, C., 2009. A concentration-dependent endocytic trap and sink mechanism converts Bmper from an activator to an inhibitor of Bmp signaling. J. Cell Biol. 184, 597–609.
Kobayashi, A., Valerius, M.T., Mugford, J.W., Carroll, T.J., Self, M., Oliver, G., McMahon, A.P., 2008. Six2 defines and regulates a multipotent self-renewing nephron progenitor population throughout mammalian kidney development. Cell Stem Cell 3, 169–181.
Korchynskyi, O., ten Dijke, P., 2002. Identification and functional characterization of distinct critically important bone morphogenetic protein-specific response elements in the Id1 promoter. J. Biol. Chem. 277, 4883–4891.
Lamb, T.M., Knecht, A.K., Smith, W.C., Stachel, S.E., Economides, A.N., Stahl, N., Yancopolous, G.D., Harland, R.M., 1993. Neural induction by the secreted polypeptide noggin. Science 262, 713–718.
Larrain, J., Oelgeschlager, M., Ketpura, N.I., Reversade, B., Zakin, L., De Robertis, E.M., 2001. Proteolytic cleavage of Chordin as a switch for the dual activities of twisted gastrulation in BMP signaling. Development 128, 4439–4447.
Lin, J., Patel, S.R., Cheng, X., Cho, E.A., Levitan, I., Ullenbruch, M., Phan, S.H., Park, J.M., Dressler, G.R., 2005. Kielin/chordin-like protein, a novel enhancer of BMP signaling, attenuates renal fibrotic disease. Nat. Med. 11, 387–393.
Luo, G., Hofmann, C., Bronckers, A.L., Sohocki, M., Bradley, A., Karsenty, G., 1995. BMP-7 is an inducer of nephrogenesis, and is also required for eye development and skeletal patterning. Genes Dev. 9, 2808–2820.
Megason, S.G., McMahon, A.P., 2002. A mitogen gradient of dorsal midline Wnts organizes growth in the CNS. Development 129, 2087–2098.
Moser, M., Binder, O., Wu, Y., Aitsebaomo, J., Ren, R., Bode, C., Bautch, V.L., Conlon, F.L., Patterson, C., 2003. BMPER, a novel endothelial cell precursor-derived protein, antagonizes bone morphogenetic protein signaling and endothelial cell differentiation. Mol. Cell. Biol. 23, 5664–5679.
Moser, M., Yu, Q., Bode, C., Xiong, J.W., Patterson, C., 2007. BMPER is a conserved regulator of hematopoietic and vascular development in zebrafish. J. Mol. Cell. Cardiol. 43, 243–253.
Nosaka, T., Morita, S., Kitamura, H., Nakajima, H., Shibata, F., Morikawa, Y., Kataoka, Y., Ebihara, Y., Kawashima, T., Itoh, T., Ozaki, K., Senba, E., Tsuji, K., Makishima, F., Yoshida, N., Kitamura, T., 2003. Mammalian twisted gastrulation is essential for skeleto-lymphogenesis. Mol. Cell. Biol. 23, 2969–2980.
Oelgeschlager, M., Larrain, J., Geissert, D., De Robertis, E.M., 2000. The evolutionarily conserved BMP-binding protein twisted gastrulation promotes BMP signalling. Nature 405, 757–763.
Oxburgh, L., Chu, G.C., Michael, S.K., Robertson, E.J., 2004. TGFbeta superfamily signals are required for morphogenesis of the kidney mesenchyme progenitor population. Development 131, 4593–4605.
Petryk, A., Anderson, R.M., Jarcho, M.P., Leaf, I., Carlson, C.S., Klingensmith, J., Shawlot, W., O'Connor, M.B., 2004. The mammalian twisted gastrulation gene functions in foregut and craniofacial development. Dev. Biol. 267, 374–386.
Rentzsch, F., Zhang, J., Kramer, C., Sebald, W., Hammerschmidt, M., 2006. Crossveinless 2 is an essential positive feedback regulator of Bmp signaling during zebrafish gastrulation. Development 133, 801–811.
Ross, J.J., Shimmi, O., Vilmos, P., Petryk, A., Kim, H., Gaudenz, K., Hermanson, S., Ekker, S.C., O'Connor, M.B., Marsh, J.L., 2001. Twisted gastrulation is a conserved extracellular BMP antagonist. Nature 410, 479–483.
Sasai, Y., Lu, B., Steinbeisser, H., Geissert, D., Gont, L.K., De Robertis, E.M., 1994. Xenopus chordin: a novel dorsalizing factor activated by organizer-specific homeobox genes. Cell 79, 779–790.
Sasai, Y., Lu, B., Steinbeisser, H., De Robertis, E.M., 1995. Regulation of neural induction by the Chd and Bmp-4 antagonistic patterning signals in Xenopus. Nature 376, 333–336.
Scott, I.C., Blitz, I.L., Pappano, W.N., Maas, S.A., Cho, K.W., Greenspan, D.S., 2001. Homologues of twisted gastrulation are extracellular cofactors in antagonism of BMP signalling. Nature 410, 475–478.
Serpe, M., Umulis, D., Ralston, A., Chen, J., Olson, D.J., Avanesov, A., Othmer, H., O'Connor, M.B., Blair, S.S., 2008. The BMP-binding protein Crossveinless 2 is a short-range, concentration-dependent, biphasic modulator of BMP signaling in Drosophila. Dev. Cell 14, 940–953.
Shah, M.M., Sampogna, R.V., Sakurai, H., Bush, K.T., Nigam, S.K., 2004. Branching morphogenesis and kidney disease. Development 131, 1449–1462.
Simic, P., Vukicevic, S., 2005. Bone morphogenetic proteins in development and homeostasis of kidney. Cytokine Growth Factor Rev. 16, 299–308.
Smith, W.C., Harland, R.M., 1992. Expression cloning of noggin, a new dorsalizing factor localized to the Spemann organizer in Xenopus embryos. Cell 70, 829–840.
Umulis, D., O'Connor, M.B., Blair, S.S., 2009. The extracellular regulation of bone morphogenetic protein signaling. Development 136, 3715–3728.
Vainio, S., Lin, Y., 2002. Coordinating early kidney development: lessons from gene targeting. Nat. Rev. Genet. 3, 533–543.
Zakin, L., De Robertis, E.M., 2004. Inactivation of mouse twisted gastrulation reveals its role in promoting Bmp4 activity during forebrain development. Development 131, 413–424.
Zakin, L., Reversade, B., Kuroda, H., Lyons, K.M., De Robertis, E.M., 2005. Sirenomelia in Bmp7 and Tsg compound mutant mice: requirement for Bmp signaling in the development of ventral posterior mesoderm. Development 132, 2489–2499.
Zakin, L., Metzinger, C.A., Chang, E.Y., Coffinier, C., De Robertis, E.M., 2008. Development of the vertebral morphogenetic field in the mouse: interactions between Crossveinless-2 and twisted gastrulation. Dev. Biol. 323, 6–18.
Zhang, J.L., Huang, Y., Qiu, L.Y., Nickel, J., Sebald, W., 2007. von Willebrand factor type C domain-containing proteins regulate bone morphogenetic protein signaling through different recognition mechanisms. J. Biol. Chem. 282, 20002–20014.
Zhang, J.L., Qiu, L.Y., Kotzsch, A., Weidauer, S., Patterson, L., Hammerschmidt, M., Sebald, W., Mueller, T.D., 2008. Crystal structure analysis reveals how the Chordin family member crossveinless 2 blocks BMP-2 receptor binding. Dev. Cell 14, 739–750.

Hes1 immortalizes committed progenitors and plays a role in blast crisis transition in chronic myelogenous leukemia

Fumio Nakahara,[1-4] Mamiko Sakata-Yanagimoto,[1,2,5] Yukiko Komeno,[3,4] Naoko Kato,[3,4] Tomoyuki Uchida,[3,4] Kyoko Haraguchi,[1,6] Keiki Kumano,[1,2] Yuka Harada,[7] Hironori Harada,[8] Jiro Kitaura,[3,4] Seishi Ogawa,[9] Mineo Kurokawa,[1,2] Toshio Kitamura,[3,4] and Shigeru Chiba[1,5]

[1]Department of Cell Therapy and Transplantation Medicine and [2]Department of Hematology Oncology, University of Tokyo, Tokyo; [3]Division of Cellular Therapy, Advanced Clinical Research Center, University of Tokyo, Tokyo; [4]Division of Stem Cell Signaling, Center for Stem Cell Therapy, Institute of Medical Science, University of Tokyo, Tokyo; [5]Department of Clinical and Experimental Hematology, Graduate School of Comprehensive Human Sciences, University of Tsukuba, Ibaraki; [6]Division of Transfusion and Cell Therapy, Tokyo Metropolitan Cancer and Infectious Disease Center Komagome Hospital, Tokyo; [7]International Radiation Information Center, Hiroshima University, Hiroshima; [8]Department of Hematology and Oncology, Research Institute for Radiation Biology and Medicine, Hiroshima University, Hiroshima; and [9]Cancer Genomics Project, Graduate School of Medicine, University of Tokyo, Tokyo, Japan

Hairy enhancer of split 1 (Hes1) is a basic helix-loop-helix transcriptional repressor that affects differentiation and often helps maintain cells in an immature state in various tissues. Here we show that retroviral expression of Hes1 immortalizes common myeloid progenitors (CMPs) and granulocyte-macrophage progenitors (GMPs) in the presence of interleukin-3, conferring permanent replating capability on these cells. Whereas these cells did not develop myeloproliferative neoplasms when intravenously administered to irradiated mice, the combination of Hes1 and BCR-ABL in CMPs and GMPs caused acute leukemia resembling blast crisis of chronic myelogenous leukemia (CML), resulting in rapid death of the recipient mice. On the other hand, BCR-ABL alone caused CML-like disease when expressed in c-Kit-positive, Sca-1-positive, and lineage-negative hematopoietic stem cells (KSLs), but not committed progenitors CMPs or GMPs, as previously reported. Leukemic cells derived from Hes1 and BCR-ABL-expressing CMPs and GMPs were more immature than those derived from BCR-ABL-expressing KSLs. Intriguingly, Hes1 was highly expressed in 8 of 20 patients with CML in blast crisis, but not in the chronic phase, and dominant negative Hes1 retarded the growth of some CML cell lines expressing Hes1. These results suggest that Hes1 is a key molecule in blast crisis transition in CML. (*Blood.* 2010;115(14):2872-2881)

Introduction

The balance between activator and repressor basic helix-loop-helix transcription factors is crucial for the proper timing of cellular differentiation and normal morphogenesis of various tissues.[1] During embryogenesis, the basic helix-loop-helix protein hairy enhancer of split 1 (Hes1), functioning downstream of the Notch receptor,[2,3] blocks differentiation of neural stem cells by antagonizing Mash1[4] and affects the cell-fate decision of pancreatobiliary epithelial progenitors.[5] In the adult hematopoietic system, Hes1 blocks granulocyte colony-stimulating factor-induced granulocytic differentiation of the 32D cell line,[6] preserving the long-term reconstituting ability of hematopoietic stem cells (HSCs) in vitro as well as in vivo.[7] Hes1 also plays a significant role in the development of perinatal T cells,[8,9] and knocking out Hes1 leads to lack of thymus.[9]

Recently, activating mutations of the *Notch1* and *Notch2* genes have been identified in more than 50% of human T-cell acute lymphoblastic leukemias[10] and in a subset of non-Hodgkin lymphomas,[11] respectively, implicating Notch signal deregulation based on a genetic abnormality in human cancers. The effect of Notch signal aberration, however, has been largely confined to lymphoid lineages in the hematopoietic compartment. Indeed, enhanced Notch signaling provides the bone-marrow-to-thymus transition stage of early progenitors, with strong selective pressure toward thymic T-cell precursors at the expense of B-cell and myeloid precursors.[12-14] We recently found that up-regulation of Hes1 represents only a part of Notch signaling during the decision between mast cell and granulocyte lineage differentiation. Notch signaling does promote mast-cell development at the expense of granulocyte differentiation through up-regulation of both Hes1 and GATA-3 in common myeloid progenitors (CMPs) and granulocyte-macrophage progenitors (GMPs). However, up-regulation of Hes1 alone causes expansion of cells with myeloid progenitor phenotypes, rather than mast cell development, mediated through down-regulation of a transcription factor, C-enhancer binding protein α (C/EBP-α).[15]

A growing volume of evidence shows that down-regulation of C/EBP-α represents major events in human acute myelogenous leukemia (AML), through either genetic or epigenetic abnormalities. Therefore, it is postulated that Hes1 up-regulation may be involved in a subset of myeloid leukemias.

Chronic myelogenous leukemia (CML) is a myeloproliferative neoplasm that originates in an abnormal pluripotent bone marrow stem cell and is consistently associated with the *BCR-ABL* fusion gene. The disease is biphasic or triphasic; an initial indolent chronic phase is followed by one or both of the aggressive stages, the accelerated phase and blast crisis, resulting in expansion of immature leukemic cells. The mainstay of chronic phase to blast

Submitted May 19, 2009; accepted September 27, 2009. Prepublished online as *Blood* First Edition paper, October 27, 2009; DOI 10.1182/blood-2009-05-222836.

The online version of this article contains a data supplement.

The publication costs of this article were defrayed in part by page charge payment. Therefore, and solely to indicate this fact, this article is hereby marked "advertisement" in accordance with 18 USC section 1734.

crisis transition is the differentiation block by additional genetic events in progenitor stages of CML cells[16] that could otherwise differentiate during the chronic phase. Thus, the transformation of BCR-ABL-induced myeloproliferative neoplasm to full-blown blast crisis has been drawing tremendous attention from investigators.

Here we show that retroviral expression of Hes1 immortalizes CMPs and GMPs in vitro. Hes1 introduction together with BCR-ABL into CMPs and GMPs, the postulated origin of blast crisis transition in CML, induced CML blast crisis-like disease when intravenously administered to sublethally irradiated mice. Considering as well the study of Hes1 expression in CML patients, we propose that Hes1 is a unique experimental tool for studying the mechanisms of chronic phase to blast crisis transformation in CML.

Methods

Mice

C57BL/6 (Ly5.1) donor mice were purchased from Sankyo Labo Service Corporation. C57BL/6 (Ly5.2) recipient mice were purchased from SLC. Mice were kept at the Animal Center for Biomedical Research, University of Tokyo, according to institutional guidelines.

Bone marrow progenitor sort

Bone marrow cells were isolated from the femurs and tibias of C57BL/6 (Ly5.1) donor mice (8-10 weeks of age) and were incubated with biotinylated antibodies for lineage markers, including anti-CD3, anti-CD4, anti-CD8, anti-B220, anti-Ter119, and anti–Gr-1 antibodies (BD Biosciences PharMingen) followed by incubation with streptavidin Micro Beads (Miltenyi Biotec). The lineage marker-negative (Lin^-) fraction was separated with an autoMACS separator or LS Columns (Miltenyi Biotec) and incubated with anti-CD34–fluorescein isothiocyanate, anti-CD16/32 (FcγRIII/II receptor)–phycoerythrin (PE), anti–c-Kit–allophycocyanin, streptavidin peridinin chlorophyll protein (BD Biosciences PharMingen), and anti–Sca-1–PE/Cy7 (eBioscience). Lin^-c-Kit^+Sca-1^+, Lin^-c-Kit^+Sca-$1^-$$Fc\gamma R^{lo}CD34^+$, and Lin^-c-Kit^+Sca-$1^-$$Fc\gamma R^{hi}CD34^+$ cells (KSLs, CMPs, and GMPs, respectively)[17] were sorted with a FACSAria cell sorter (BD Biosciences).

Transfection and retrovirus production for murine cells

Rat Hes1 cDNA, a gift from R. Kageyama (Kyoto University, Kyoto, Japan), was subcloned into a retrovirus vector, GCDNsam/internal ribosome entry site (IRES)–nerve growth factor receptor (NGFR), a gift from H. Nakauchi (University of Tokyo) and M. Onodera (National Center for Child Health and Development, Tokyo, Japan). BCR-ABL (p210) cDNA[18] was subcloned into a retrovirus vector, GCDNsam/IRES-GFP.[19] Mouse C/EBP-α cDNA, a gift from K. Akashi (Kyushu University, Fukuoka, Japan) and S. Mizuno (Dana-Farber Cancer Institute, Boston, MA), was subcloned into a retrovirus vector, pMYs-IRES-GFP.[19] Plat-E[20] packaging cells maintained in Dulbecco modified Eagle medium supplemented with 10% fetal calf serum were transfected with retroviral constructs using FuGENE 6 transfection reagent (Roche Diagnostics) according to the manufacturer's instructions. The medium was changed a day after transfection, and retroviruses were harvested 48 hours after transfection, as previously described.[19,20]

Transfection and retrovirus production for human cell lines

We generated a dominant-negative Hes1 (dnHes1) lacking a C-terminal WRPW (Trp-Arg-Pro-Trp) domain as described.[21] The fragment of dnHes1 was subcloned into pMYs-IRES-GFP.[19] Retrovirus packaging was done as described. Briefly, retroviruses were generated by transient transfection of Plat-A[20] packaging cells with FuGENE 6 (Roche Diagnostics).

Infection to progenitors

The retrovirus medium was placed in 24-well nontissue culture dishes for 4 hours at 37°C, precoated with 40 μg/mL of RetroNectin (Takara Bio) overnight at 4°C. After washing the wells with phosphate-buffered saline, sorted KSLs, CMPs, or GMPs were plated for infection for 48 to 60 hours with the coated retroviruses harboring GCDNsam/IRES-GFP-BCR-ABL (p210) or GCDNsam/IRES-NGFR-Hes1 or an empty vector as a control. Infection was done in StemSpan SFEM medium (StemCell Technologies) containing 100 ng/mL mouse stem cell factor (SCF), 100 ng/mL mouse thrombopoietin (TPO), and 100 ng/mL human FLT3 ligand (FL) for KSLs, or in Iscove modified Dulbecco medium (Sigma-Aldrich) containing 20% fetal calf serum, 50 ng/mL mouse SCF, 20 ng/mL mouse TPO, and 20 ng/mL mouse interleukin-3 (IL-3), 20 ng/mL human IL-6 (R&D Systems) for CMPs or GMPs.

Colony-forming assay

Retrovirus-infected cells were sorted at 48 to 60 hours from the initiation of infection with a FACSAria cell sorter (BD Biosciences) and used for colony-forming assay using Methocult 3231 (StemCell Technologies), supplemented with 50 ng/mL mouse SCF, 20 ng/mL mouse TPO, and 20 ng/mL mouse IL-3, 20 ng/mL human IL-6. A total of 1000 cells were cultured in each 2.5-cm dish in duplicate. The colony-forming cells were harvested and replated every 7 to 9 days and scored for colony formation. We defined a colony as "a group of cells, grown from a single parent cell, which is composed of more than 40 live cells."

Mouse bone marrow transplantation

Bone marrow cells prepared from C57BL/6-Ly5.1 mice were infected with retrovirus containing Hes1 or BCR-ABL, and 0.1 to 2.6×10^5 of Hes1/NGFR-sorted or BCR-ABL/GFP-sorted cells were injected through tail veins into C57BL/6-Ly5.2-recipient mice (8-12 weeks of age) after sublethal (5.25 Gy) or lethal (9.5 Gy) total body γ-irradiation (^{135}Cs). For the lethally irradiated mice, 2×10^5 of C57BL/6-Ly5.2 mice-derived bone marrow cells were simultaneously injected for radioprotection. Probabilities of overall survival of the mice that received transplantations were estimated using the Kaplan-Meier method. Statistical differences were determined by the Wilcoxon test. All animal studies were approved by the Animal Care Committee of the Institute of Medical Science, University of Tokyo.

Analysis of mice receiving transplantation

After transplantation, mice were monitored for signs of disease, such as cachexia, hyperpnea, or loss of gloss in fur. Autopsies were performed on moribund recipient mice. Peripheral blood count was analyzed by KX-21 Auto Analyzer (Sysmex). Morphology of the peripheral blood was evaluated by staining of air-dried smears with Hemacolor (Merck). Tissues including bone marrow, spleen, and liver were fixed in 10% buffered formalin, embedded in paraffin, sectioned, and stained with hematoxylin and eosin. Cytospin preparations of bone marrow and spleen cells were also stained with Hemacolor. Percentage of blasts, myelocytes, neutrophils, monocytes, lymphocytes, and erythroblasts was estimated by examination of at least 200 cells. To assess whether the leukemic cells were transplantable to secondary recipients, 0.1 to 5×10^6 total bone marrow cells were injected into the tail veins of sublethally irradiated mice. Two recipient mice were used for each serial transplantation.

Flow cytometric analysis

Red blood cells were lysed using Red Blood Cell Lysing Buffer (Sigma-Aldrich) in peripheral blood or single-cell suspensions of bone marrow and spleen. After washing with phosphate-buffered saline, Fc receptor was blocked by incubating cells with 2.4G2 antibody (eBioscience) for 15 minutes at 4°C and then staining them with the following PE-conjugated monoclonal antibodies for 20 minutes at 4°C: Ly-5.1, Gr-1, CD11b, B220, CD19, CD3, CD4, CD8, c-Kit, Sca-1, CD34, and Ter119. Flow-cytometric analysis of the stained cells was performed with FACSCalibur

(BD Biosciences) equipped with CellQuest software (BD Biosciences) and FlowJo software (TreeStar).

Patients

CML patients were diagnosed at Hiroshima University Hospital and its affiliated hospitals. Diagnosis was based on morphologic, immunophenotypic, and, in some cases, real-time reverse transcription-polymerase chain reaction (RT-PCR) studies according to the French-American-British classification or World Health Organization classification. Patient samples were prepared after the research plan was approved by the Institutional Review Board at Hiroshima University, and written informed consent was obtained in accordance with the Declaration of Helsinki. Investigations were carried out in accordance with ethical standards authorized by the ethics committee of Hiroshima University and the ethics committee of the University of Tokyo (approval no. 20-10-0620)

Real-time RT-PCR

Total RNA was extracted from human bone marrow or peripheral blood cells using a TRIzol Kit (Invitrogen) according to the manufacturer's instructions, and converted to cDNA with a High Capacity cDNA Reverse Transcription Kit (Applied Biosystems). Total RNA of mouse progenitors was extracted with RNeasy (QIAGEN) according to the manufacturer's instructions, and converted to cDNA with a High Capacity cDNA Reverse Transcription Kit (Applied Biosystems). Real-time RT-PCR was performed using a LightCycler Workflow System (Roche Diagnostics). cDNA was amplified using a SYBR Premix EX Taq (Takara). Reaction was subjected to 1 cycle of 95°C for 30 seconds, 45 cycles of PCR at 95°C for 5 seconds, 58°C for 10 seconds, and 72°C for 10 seconds. All samples were independently analyzed at least 3 times. The following primer pairs were used: 5′-CCAGTTTGCTTTCCTCATTCC-3′ (forward) and 5′-TCTTCTCTCCCAGTATTCAAGTTCC-3′ (reverse) for human Hes1[22]; 5′-GAGCTGAACGGGAAGCTCACTGG-3′ (forward) and 5′-CAACTGTGAGGAGGGGAGATTCAG-3′ (reverse) for human GAPDH[22]; 5′-GAACAGCAACGAGTACCGGGTA-3′ (forward) and 5′-CCCATGGCCTTGACCAAGGAG-3′ (reverse) for mouse C/EBP-α[23]; 5′-CACAGGACTAGAACACCTGC-3′ (forward) and 5′-GCTGGTGAAAAGGACCTCT-3′ (reverse) for mouse hypoxanthine phosphoribosyltransferase (HPRT).[23] Relative gene expression levels were calculated using standard curves generated by serial dilutions of cDNA. Product quality was checked by melting curve analysis via LightCycler software (Roche Diagnostics). Expression levels were normalized by a control, the expression level of GAPDH mRNA for human samples, and HPRT mRNA for mouse samples.

Western blot analysis

To detect the expression of Hes1 or BCR-ABL (p210) proteins, equal numbers of cells from spleen or cell line were lysed, and Western blotting was performed as described with minor modifications.[24] Polyclonal rabbit anti-Hes1 antibody (H-140; Santa Cruz Biotechnology) and polyclonal rabbit anti–c-ABL antibody (K-12; Santa Cruz Biotechnology) were used for Hes1 or BCR-ABL detection, respectively.

Results

Retroviral transduction of Hes1 immortalizes CMPs and GMPs

NGFR-sorted Hes1-transduced KSLs, CMPs, and GMPs similarly generated compact and relatively large colonies, whereas empty vector-transduced KSLs generated a similar number of less large colonies. Empty vector-transduced CMPs and GMPs did not generate colonies (Figure 1A). Cytospin preparations of Hes1-transduced progenitors, stained with Hemacolor (Merck), showed blast-like morphologies, whereas those of empty vector-transduced KSLs contained bands, macrophages, and blasts (Figure 1B). Most of the empty vector-transduced CMPs and GMPs died and few cells remained (Figure 1B). In serial colony-forming assays, both CMPs and GMPs transduced with Hes1 formed colonies after at least 4 rounds of replating, with the plating efficiency more than 15% at the fourth round (Figure 1C). Replating could be reproducibly maintained for more than half a year, implying immortalizing activity of Hes1 (Figure 1D). The Hes1-transduced KSLs, CMPs, and GMPs were dependent on the presence of IL-3, requiring concentrations more than 1 ng/mL (Figure 1E; supplemental Figure 1A-B, available on the *Blood* website; see the Supplemental Materials link at the top of the online article). There was no significant difference between these cells in the dependency on IL-3. The majority of Hes1-transduced cells expressed c-Kit and CD34 at high levels, Sca-1 and CD11b at intermediate levels (Figure 1F, supplemental Figure 2A-B), irrespective of whether they were derived from KSLs, CMPs, or GMPs (supplemental Figure 2E).

The Lin^- cells were further analyzed by adopting 5-color flow cytometry that is used to identify bone marrow KSLs, CMPs, and GMPs. The expression levels of c-Kit, Sca-1, and CD34 were distributed over wide ranges. Approximately 2.5% to 6.4% of all nucleated cells showed a phenotype similar to KSLs, and another 4.8% to 11.6% showed a phenotype similar to GMPs. There were few cells that resembled CMPs (Figure 1G). We sorted the KSL-like cells, CMP-like cells, and GMP-like cells from each Hes1-transduced cell (Hes1-KSLs, Hes1-CMPs, and Hes1-GMPs) and cultured them for a week in methylcellulose. The same analysis by 5-color flow cytometry showed accumulation of GMP-like cells (~ 45.3%-83.5% of all nucleated cells) and moderate accumulation of KSL-like cells (~ 4.3%-23.4% of all nucleated cells) in the cultured cells (supplemental Figure 3A-C).

BCR-ABL replaces IL-3 in Hes1-immortalized cell lines

Because the Hes1-immortalized cell lines were IL-3 dependent for their growth in vitro, we examined whether additional signaling could replace IL-3. IL-3 signaling takes place mainly via Stat-, Ras-MAPK-, and PI3K-Akt-dependent pathways. It is also known that CML-specific BCR-ABL (p210) can replace IL-3 signaling in several experimental designs. Thus, we retrovirally expressed BCR-ABL together with Hes1. The combination of Hes1 and BCR-ABL enabled KSLs, CMPs, and GMPs to form colonies after repeated replating, not only in the presence of cytokines (Figure 2A left panel) but also in the condition free from cytokines (Figure 2A right panel). In contrast, KSLs, but not CMPs or GMPs, formed colonies by BCR-ABL transduction alone only when supplemented with cytokines (Figure 2A left panel), and they did not form any colonies without cytokines (Figure 2A right panel) or after replating with/without cytokines (Figure 2A both panels). In the liquid culture, it was shown that KSLs, CMPs, and GMPs transduced with both Hes1 and BCR-ABL were immortalized without cytokine supplementation (Figure 2B). The colonies made from Hes1- and BCR-ABL-transduced cells showed similar morphology with those from Hes1-transduced cells in the presence of a cytokine cocktail (Figure 2C). Importantly, the morphology of colony-forming cells derived from BCR-ABL-transduced KSLs was much more mature compared with those derived from Hes1- and BCR-ABL-transduced KSLs, CMPs, and GMPs, even in the same cytokine cocktail (Figure 2D). The majority of $Hes1^+$BCR-ABL^+ KSLs as well as $Hes1^+$BCR-ABL^+ CMPs and GMPs expressed CD34 at high levels, whereas they expressed c-Kit, Sca-1, and CD11b at intermediate levels (Figure 2E; supplemental Figure 2C-D), irrespective of whether they were derived from

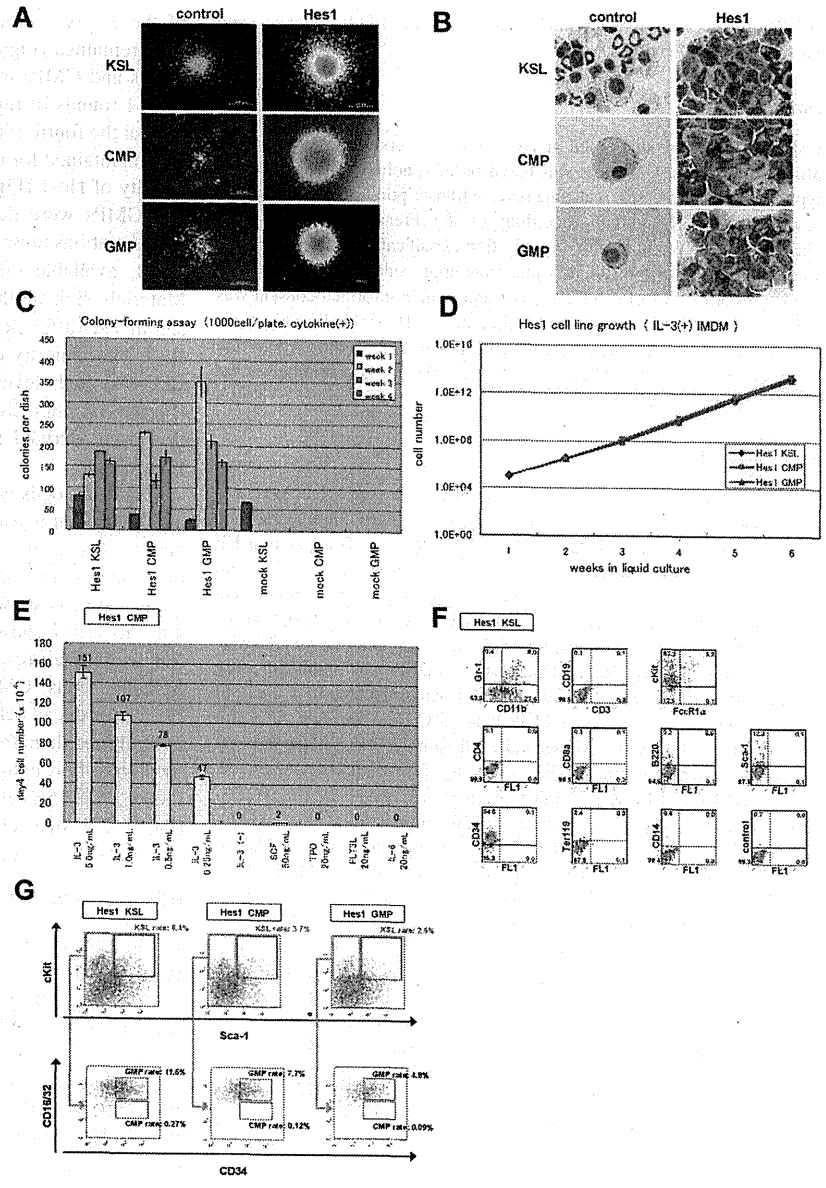

Figure 1. Hes1-transduced KSLs, CMPs, or GMPs were immortalized in the presence of IL-3. (A) Typical colonies derived from Hes1- and empty vector-transduced KSLs, CMPs, and GMPs in the presence of SCF, TPO, IL-3, and IL-6. Images were obtained with an IX70 microscope and a DP70 camera (Olympus); an objective lens, UPlanFI (Olympus); original magnification ×40 (bottom 2 in the right panels) and original magnification ×100 (remaining 4 panels). (B) Giemsa staining of Hes1- and control vector-transduced KSLs, CMPs, and GMPs. Images were obtained with a BX51 microscope and a DP12 camera (Olympus); an objective lens, UPlanFI (Olympus); original magnification ×1000. (C) Colony-forming assay from KSLs, CMPs, and GMPs transduced with Hes1 or empty vector. Hes1-transduced cells were replatable more than 4 times in vitro. Bars represent the number of colonies obtained per 10^3 cells after each round of plating in methylcellulose supplemented with SCF, TPO, IL-3, and IL-6. A representative result from 3 independent and reproducible experiments is shown. Error bars represent the SD from duplicate cultures. (D) Sustained growth of Hes1-transduced cells in liquid culture supplemented with 1 ng/mL IL-3. The number of cells was determined every 7 days by trypan blue staining, and 10^5 cells per well were seeded into a 6-well plate. Liquid culture was reproducibly continued for more than 6 months. (E) Cytokine requirement of Hes1-transduced CMPs. The cells were cultured in Iscove modified Dulbecco medium supplemented with indicated cytokines in duplicate. The numbers of cells were counted after 4 days of culture. A representative result from 2 independent and reproducible experiments is shown. Error bars represent the SD from duplicate cultures. Hes1-transduced KSLs and GMPs showed similar results (supplemental Figure 1A-B). (F) Flow-cytometric analysis of Hes1-transduced KSLs cultured in methylcellulose supplemented with SCF, TPO, IL-3, and IL-6. The dot plots represent Gr-1, CD19, c-Kit, CD4, CD8a, B220, Sca-1, CD34, Ter119, and CD14 labeled with a corresponding PE-conjugated monoclonal antibody versus CD11b, CD3, and FcεR1α labeled with a corresponding fluorescein isothiocyanate-conjugated monoclonal antibody or FL1 with no monoclonal antibody. Hes1-transduced CMPs and GMPs showed similar expression patterns (supplemental Figure 2A-B). (G) Flow-cytometric analysis of Lin⁻-gated Hes1-transduced cells. Five-color analyses are used to identify KSL-like (top panels) and CMP-like and GMP-like cells (bottom panels) in the Hes1-transduced KSLs, CMPs, and GMPs. The number shows the percentage of cells in all nucleated cells. The analyzed cells were NGFR sorted at 48 to 60 hours from the initiation of Hes1- or control vector-transduction and cultured for the following lengths of time before the analysis: (A) 1 week, (B) 1 week, (C) 0 days, (D) 4 weeks, (E) 2 weeks, (F) 1 week, and (E) 2 weeks.

KSLs, CMPs, or GMPs (supplemental Figure 2F). Hes1$^+$BCR-ABL$^+$ KSLs, CMPs, and GMPs showed lower expressions of c-Kit and CD34 than KSLs, CMPs, and GMPs transduced with Hes1 alone (supplemental Figure 2E-F) when cultured in the presence of the same cytokine cocktail (SCF, TPO, IL-3, and IL-6). Expression of Hes1 or BCR-ABL in the Hes1 ± BCR-ABL transduced CMP or GMP cell lines was confirmed by Western blot analysis (supplemental Figure 4A).

Hes1$^+$BCR-ABL$^+$ CMPs and GMPs rapidly induce AML/CML blast crisis-like disease in recipient mice

To examine the effect of Hes1 on leukemogenesis, Hes1-transduced KSLs, CMPs, and GMPs were injected through tail veins into C57BL/6-Ly5.2 recipient mice (8-12 weeks of age) after a sublethal (5.25 Gy) or a lethal (9.5 Gy) dose of total-body γ-irradiation (^{135}Cs). For the lethally irradiated mice, 2×10^5 bone marrow cells from C57BL/6-Ly5.2 mice were simultaneously injected for radioprotection. All the mice that received transplantations of Hes1-transduced KSLs, CMPs, and GMPs were kept healthy, and no recipients developed myeloproliferative neoplasms (MPNs) or leukemias for up to 250 days after the transplantation (Figure 3A). Regarding the nonleukemogenic nature of the stem/progenitor cells transduced with Hes1 alone, we[7] and others[25] previously reported similar results, although the cell populations and/or experimental designs were not identical.

In agreement with the previous reports,[26] recipient mice injected with BCR-ABL-transduced KSLs developed fatal MPN within 30 days after the transplantation, whereas those injected with BCR-ABL-transduced CMPs and GMPs were kept healthy for more than 130 days. We did not find any signs of MPN or leukemias when mice were killed between 130 and 200 days after the transplantation (Figure 3B).

Because we found that the combination of Hes1 and BCR-ABL transduction conferred cytokine-independent immortalization on CMPs and GMPs, we injected Hes1$^+$BCR-ABL$^+$ KSLs, CMPs, and GMPs through tail veins into C57BL/6-Ly5.2 recipient mice

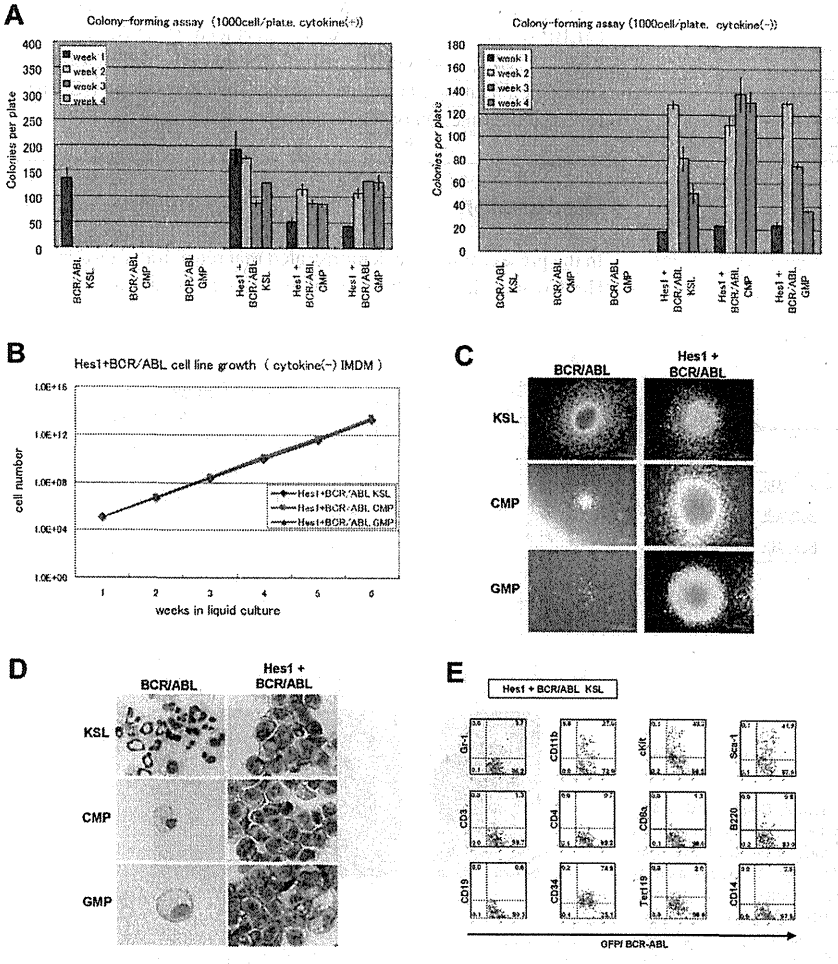

Figure 2. Hes1- and BCR-ABL-transduced KSLs, CMPs, or GMPs were immortalized independently of IL-3. (A) Colony-forming assay of KSLs, CMPs, and GMPs transduced with BCR-ABL alone or Hes1 and BCR-ABL, cultured in methylcellulose with or without cytokine cocktail containing SCF, TPO, IL-3, and IL-6. Hes1$^+$BCR-ABL$^+$ cells could be serially replated more than 4 times both with or without cytokines. In contrast, whereas KSLs, but not CMPs or GMPs, transduced with BCR-ABL alone, formed colonies in the presence of cytokines, neither KSLs, nor CMPs, nor GMPs formed colonies without cytokine supplementation. Bars represent the number of colonies obtained per 10^3 cells after each round of plating in methylcellulose. A representative result from 3 independent and reproducible experiments is shown. Error bars represent the SD from duplicate cultures. (B) Sustained growth of Hes1$^+$BCR-ABL$^+$ cells in liquid culture without cytokine supplementation. The numbers of cells were determined every 7 days by trypan blue staining, and 10^5 cells per well were seeded into a 6-well plate. Liquid culture was reproducibly continued for more than 6 months. (C) Typical colonies derived from KSLs, CMPs, and GMPs transduced with BCR-ABL alone (left panels) or BCR-ABL and Hes1 (right panels) in the presence of SCF, TPO, IL-3, and IL-6. Images were obtained with an IX70 microscope and a DP70 camera (Olympus); an objective lens, UPlanFI (Olympus); original magnification ×100. (D) Giemsa staining of Hes1$^+$BCR-ABL$^+$ KSLs, CMPs, and GMPs. Images were obtained with a BX51 microscope and a DP12 camera (Olympus); an objective lens, UPlanFI (Olympus); original magnification ×1000. (E) Flow-cytometric analysis of Hes1$^+$BCR-ABL$^+$ KSLs cultured in methylcellulose supplemented with SCF, TPO, IL-3, and IL-6. The dot plots represent Gr-1, CD11b, c-Kit, Sca-1, CD3, CD4, CD8a, B220, CD19, CD34, Ter119, and CD14 labeled with a corresponding PE-conjugated monoclonal antibody versus expression of GFP/BCR-ABL. Hes1$^+$BCR-ABL$^+$ CMPs and GMPs showed a similar expression pattern (supplemental Figure 2C-D). The analyzed cells were GFP and NGFR sorted at 48 to 60 hours from the initiation of BCR-ABL- or Hes1+BCR-ABL transduction and cultured for the following lengths of time before the analysis: (A) 0 days, (B) 4 weeks, (C) 1 week, (D) 1 week, and (E) 1 week.

after sublethal irradiation. The numbers of cells injected varied among experiments, ranging from 17×10^2 to 15×10^4, because of the difference in sorting efficiencies. All the mice receiving transplantations rapidly developed fatal AML/CML in blast crisis-like disease with no significant difference in latency, ranging between 18 and 39 days after the transplantation ($P < .867$) (Figure 4A). The tissue distribution of the disease was virtually the same among mice receiving KSLs, CMPs, and GMPs; they invariably demonstrated marked hepatosplenomegaly and lung hemorrhage resulting from infiltration of leukemic cells (Figure 4B). Expression of Hes1 and BCR-ABL in the spleen cells of recipient mice was confirmed by Western blot analysis (supplemental Figure 4B).

The morphology of bone marrow demonstrated increased myeloid blasts (Figure 4C), and the histology of spleen, liver, and lungs demonstrated extensive infiltration of leukemic cells (Figure 4D). The percentages of the blasts ranged between 28% and 55% of all nucleated bone marrow cells (mean, 36.5%) of the mice receiving Hes1- and BCR-ABL-transduced KSLs, CMPs, and GMPs. In contrast, the percentages of bone marrow blasts in the recipient mice receiving BCR-ABL-transduced KSLs were only 6% to 7% (Figure 5A). White blood cell counts in the peripheral blood of recipients with Hes1$^+$BCR-ABL$^+$ KSLs, CMPs, and GMPs were $2.4 \times 10^4/\mu L$ to $67.9 \times 10^4/\mu L$ (mean, $17.8 \times 10^4/\mu L$), whereas those with BCR-ABL-transduced KSLs showed moderate leukocytosis ranging between $2.9 \times 10^4/\mu L$ and $3.8 \times 10^4/\mu L$ (Figure 5B). The surface marker profiles of the bone marrow cells from the recipients with Hes1$^+$BCR-ABL$^+$ cells expressed CD11b and Gr-1 at high levels, whereas they expressed c-Kit, Sca-1, and CD34 at intermediate levels (Figure 5C; supplemental Figure 5A-B), irrespective of whether they were derived from KSLs, CMPs, or GMPs (supplemental Figure 5C).

The long-term self-renewal properties of the leukemic cells derived from Hes1- and BCR-ABL-transduced CMPs or GMPs were tested by transplantation into secondary recipients; 0.1 to 5×10^6 total bone marrow cells were injected into the tail veins of sublethally irradiated mice. All recipient mice transplanted with more than 10^5 Hes1$^+$ cells from bone marrow developed fatal AML/CML in blast crisis-like disease with latencies of between 18 and 75 days (supplemental Figure 4C). The disease was almost identical with the primary disease (data not shown).

Hes1 expression is elevated in a substantial subset of human CML blast crisis samples

The results presented from the mouse model experiments suggest a potential link between deregulated expression of Hes1 and human CML in blast crisis. We measured the Hes1 mRNA by real-time RT-PCR in 11 peripheral blood, 1 cerebrospinal fluid, and 8 bone marrow samples from CML in blast crisis patients; 19 bone marrow samples from CML in chronic phase patients; and 10 bone marrow samples from normal subjects. In 8 of 20 CML in blast crisis samples, we found that Hes1 mRNA levels were elevated by more than 4 times the average of normal bone marrow samples (Figure

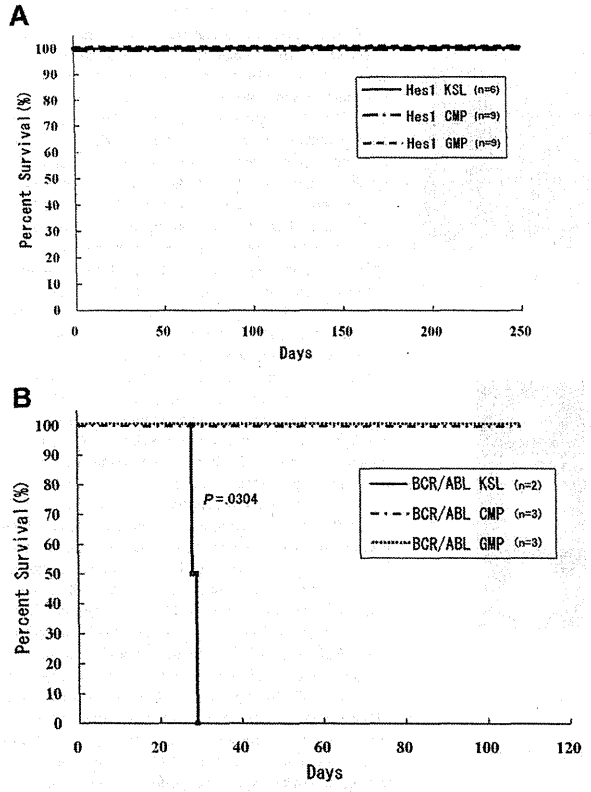

Figure 3. Mice transplanted with Hes1-transduced KSLs, CMPs, and GMPs were kept healthy. (A) Survival curves for mice injected with Hes1-transduced progenitors. No mice showed any signs of MPN for more than 250 days from transplantation. Data were analyzed by the Kaplan-Meier method. The numbers of transplanted mice are shown. Three independent experiments were performed. (B) Survival curves for mice injected with BCR-ABL-transduced progenitors. Mice transplanted with BCR-ABL-transduced KSLs developed fatal MPN within 30 days after transplantation, whereas mice transplanted with BCR-ABL-transduced CMPs or GMPs showed no evidence of disease when killed between 130 and 200 days after transplantation. Data were analyzed using the log-rank test. The 2 independent experiments were performed, and the total numbers of transplanted mice are shown.

6A). Interestingly, all but one of their phenotypes were myeloid, and 5 of 12 samples in which Hes1 mRNA levels were not elevated were derived from patients with B-cell lineage lymphoid crisis. On the other hand, the average of Hes1 mRNA levels in CML in chronic phase samples seemed to be lower than that of the normal bone marrow samples, with no sample exceeding twice the average. Clinical data of 20 patients with CML in blast crisis are shown in Table 1. The correlation coefficient between the blast percentage and the Hes1 mRNA level was −0.395, indicating that the elevated Hes1 expression level was independent of the increase in the blast percentage.

To investigate the role of Hes1 in CML blast crisis, we measured the Hes1 mRNA by real-time RT-PCR in 5 human cell lines (K-562,[27] JK-1,[28] KCL-22,[29] TS9:22,[30] and JURL-MK1[31]), which were derived from CML in blast crisis. We found that, in 3 of 5 CML blast crisis cell lines, Hes1 mRNA levels were elevated compared with the normal bone marrow sample (Figure 6B). We transduced a dominant-negative Hes1 (dnHes1) lacking a C-terminal WRPW domain via retrovirus vector into the 3 cell lines (K-562, TS9:22, and JURL-MK1) in which Hes1 mRNA levels were elevated. Indeed, in 2 of these 3 cell lines, proliferation was significantly suppressed by transduction of dnHes1 (Figure 6C). The repression of C/EBP-α by Hes1 was also observed in Hes1-transduced KSLs, CMPs, and GMPs compared with control vector-transduced KSLs, CMPs, and GMPs (Figure 6D). When C/EBP-α retrovirus vector was transduced to Hes1-transduced KSLs, CMPs, and GMPs, all of these cells differentiated to segmented neutrophils, suggesting that the expression of C/EBP-α reversed the function of Hes1 (supplemental Figure 6).

Discussion

In the present study, we demonstrated that retroviral transduction of Hes1 readily immortalizes myeloid progenitors at various stages.

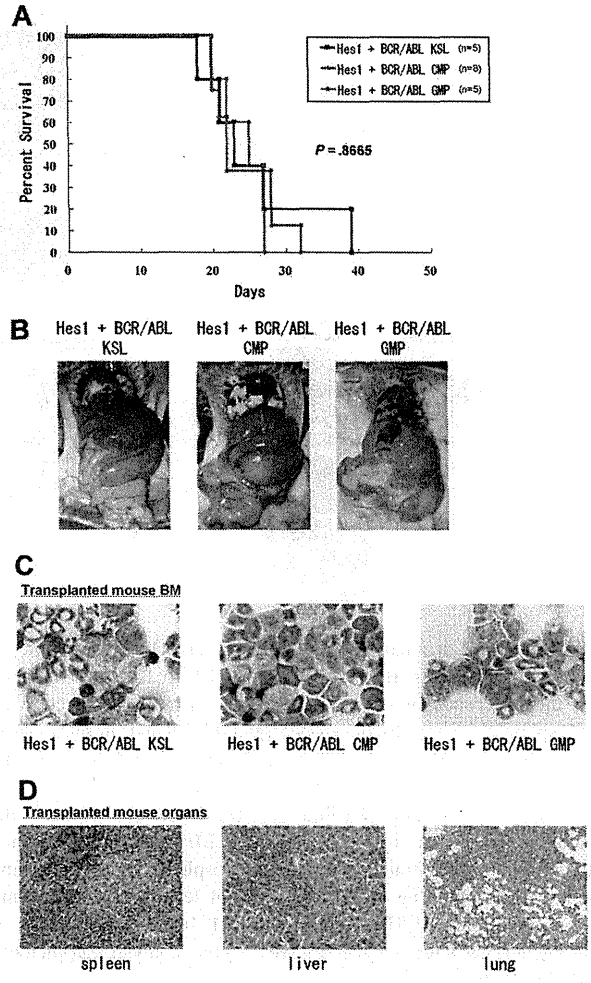

Figure 4. CMPs and GMPs transduced with the combination of Hes1 and BCR-ABL rapidly induced AML/blast crisis of CML. (A) Survival curves of mice. KSLs (n = 5), CMPs (n = 8), and GMPs (n = 5) transduced with the combination of Hes1 and BCR-ABL developed fatal AML/CML in blast crisis-like disease within 18 to 39 days, 20 to 32 days, and 20 to 27 days, respectively. Numbers of injected cells ranged 17×10^2 to 2.6×10^4 for KSLs, 5.5×10^4 to 15×10^4 for CMPs, and 4.0×10^4 to 13.8×10^4 for GMPs. There was no significant difference in latency of penetrance ($P < .867$). Statistical differences were determined using the log-rank test. Three independent experiments were performed, and the total numbers of transplanted mice are shown. (B) Tissue distribution of the leukemic cells. Mice transplanted with KSLs, CMPs, and GMPs transduced with the combination of Hes1 and BCR-ABL invariably demonstrated marked hepatosplenomegaly and lung hemorrhage, both resulting from infiltration of leukemic cells. (C) The morphology of bone marrow cells from representative recipient mice. Increased myeloid blasts were seen with no significant difference among KSLs, CMPs, and GMPs. (D) Histology of spleen, liver, and lungs from representative mice receiving Hes1$^+$BCR-ABL$^+$ GMPs. Vast infiltration of leukemic cells is seen. There were no differences in the histology among mice receiving Hes1$^+$BCR-ABL$^+$ KSLs, CMPs, and GMPs.

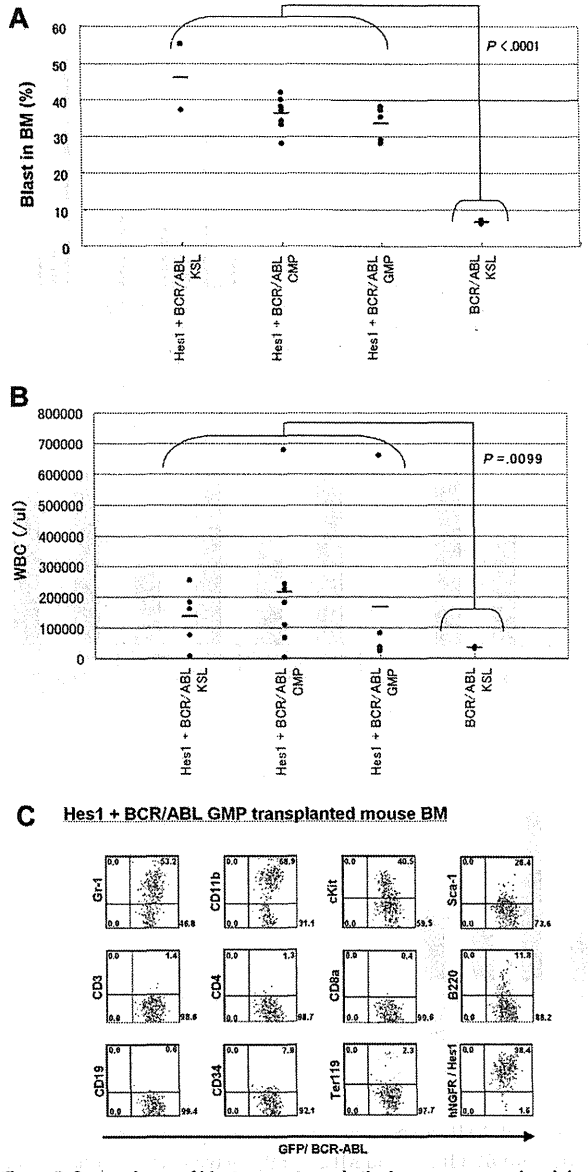

Figure 5. Comparisons of blast percentages in the bone marrow and peripheral blood leukocyte counts between mice receiving KSLs transduced with BCR-ABL alone and those receiving KSLs, CMPs, and GMPs transduced with the combination of Hes1 and BCR-ABL. (A) Blast ratios in the bone marrow. The mean blast ratios in all nucleated bone marrow cells were 6.5% ± 0.7% and 36.5% ± 6.9% in mice receiving KSLs transduced with BCR-ABL alone and in those receiving KSLs, CMPs, and GMPs transduced with the combination of Hes1 and BCR-ABL, respectively. The difference was statistically significant by the 2-sample *t* test with Welch correction ($P < .001$). (B) Peripheral white blood cell counts (WBCs). WBCs were 3.4 ± 0.6 × $10^4/\mu L$ and 17.8 ± 20.3 × $10^4/\mu L$ in mice receiving KSLs transduced with BCR-ABL alone and in those receiving KSLs, CMPs, and GMPs transduced with the combination of Hes1 and BCR-ABL, respectively. The difference was statistically significant by the 2-sample *t* test with Welch correction ($P < .001$). (C) Flow-cytometric analysis of bone marrow cells from mice receiving GMPs transduced with the combination of Hes1 and BCR-ABL. The dot plots represent Gr-1, CD11b, c-Kit, Sca-1, CD3, CD4, CD8a, B220, CD19, CD34, Ter119, and NGFR labeled with the corresponding PE-conjugated monoclonal antibody versus expression of GFP/BCR-ABL. NGFR is a marker of Hes1, and GFP is a marker of BCR-ABL transduction. The bone marrow cells derived from mice receiving KSLs or CMPs transduced with the combination of Hes1 and BCR-ABL showed essentially the same pattern (supplemental Figure 5A-B).

Moreover, when BCR-ABL is transduced together, Hes1 tranforms differentiated myeloid progenitors, such as CMPs and GMPs, in addition to hematopoietic stem cell-rich population, such as KSLs, to AML/CML in blast crisis-like cells, rapidly killing recipient mice. This result is in sharp contrast to the fact that a hematopoietic stem cell-containing population is required for BCR-ABL to cause MPN-like disease.

Hes1 is known as an effector molecule functioning downstream of Notch signaling. The activating mutations of the extracellular heterodimerization domain and/or the C-terminal PEST domain of Notch1 have been identified in approximately 50% of human T-cell acute lymphoblastic leukemias.[10,32] We have recently identified gain-of-function mutations of *Notch2* in conjunction with increased copy numbers of the mutation-carrying *Notch2* allele in a subset of B-cell lymphomas.[11] A possible association between deregulated Notch signaling is also reported in Hodgkin lymphoma, anaplastic large cell lymphoma, small-cell lung cancer, and prostate adenocarcinoma, etc.[33] Regarding myeloid malignancies, however, only one paper reports the identification of the activating mutation of Notch1 in 1 of 12 human AML samples.[34] Given that Notch signaling is among the strongest inducers of T-cell lineage commitment[12,13] and that increased Notch signaling could block myeloid lineage commitment,[15] deregulated Notch signaling might antagonize, rather than promote, the development of myeloid malignancies. However, Hes1 does not necessarily represent Notch signaling. Indeed, other extracellular signaling, such as Sonic Hedgehog,[35] could affect Hes1 expression, and cross-talk between Hes family proteins and molecules in various cell signaling pathways, such as Stat3,[36] has been demonstrated.

We previously reported that Hes1 preserved highly purified hematopoietic stem cells in vitro and contributed to the expansion of transduced hematopoietic stem cells in the recipients' bone marrow,[7] but the effect of Hes1 transduction on myeloid progenitors was not evaluated in detail. We have now found the myeloid progenitor-immortalizing activity of Hes1. In addition, accumulation of KSL- and GMP-like population in Hes1-transduced cells implicates a role for Hes1 in leukemic stem cells. On the other hand, we have also found that the in vitro growth of the Hes1-immortalized cells is dependent on cytokine signaling and that Hes1 alone is insufficient to be fully leukemogenic when overexpressed. The mainstay of the Hes1 effects on myeloid progenitors appears to be blockade of differentiation, although other functions, such as reversion from the quiescent state to the actively cycling state,[21] may also be involved. In the present study, we confirmed that Hes1 expression represses C/EBP-α, a transcription factor having important roles in myeloid differentiation, in mouse KSLs and committed progenitors as we reported.[15] Moreover, transduction of C/EBP-α reversed the differentiation block caused by Hes1 expression, which partially explains the mechanism of blocked myeloid differentiation by Hes1. C/EBP-α is frequently mutated in AML with the normal karyotype.[37-39] In other human AML without C/EBP-α mutations, reduced C/EBP-α expression, possibly through deregulated epigenetic control, is not uncommon and is associated with poor prognosis.[40,41] Furthermore, mice injected with mutated C/EBP-α-transduced bone marrow cells develop myelodysplastic syndrome and AML.[42] Therefore, reduction of C/EBP-α function is highly relevant to the development and/or progression of myeloid malignancies. Hes1, therefore, might be involved in human myeloid malignancies through suppression of C/EBP-α.

Up-regulation of Hes1 is shown in a subset of human rhabdomyosarcomas[21] and medulloblastomas.[43,44] In the present study, we have detected elevated expression of Hes1 in 8 of the 20 samples from CML in blast crisis patients, but not those from CML

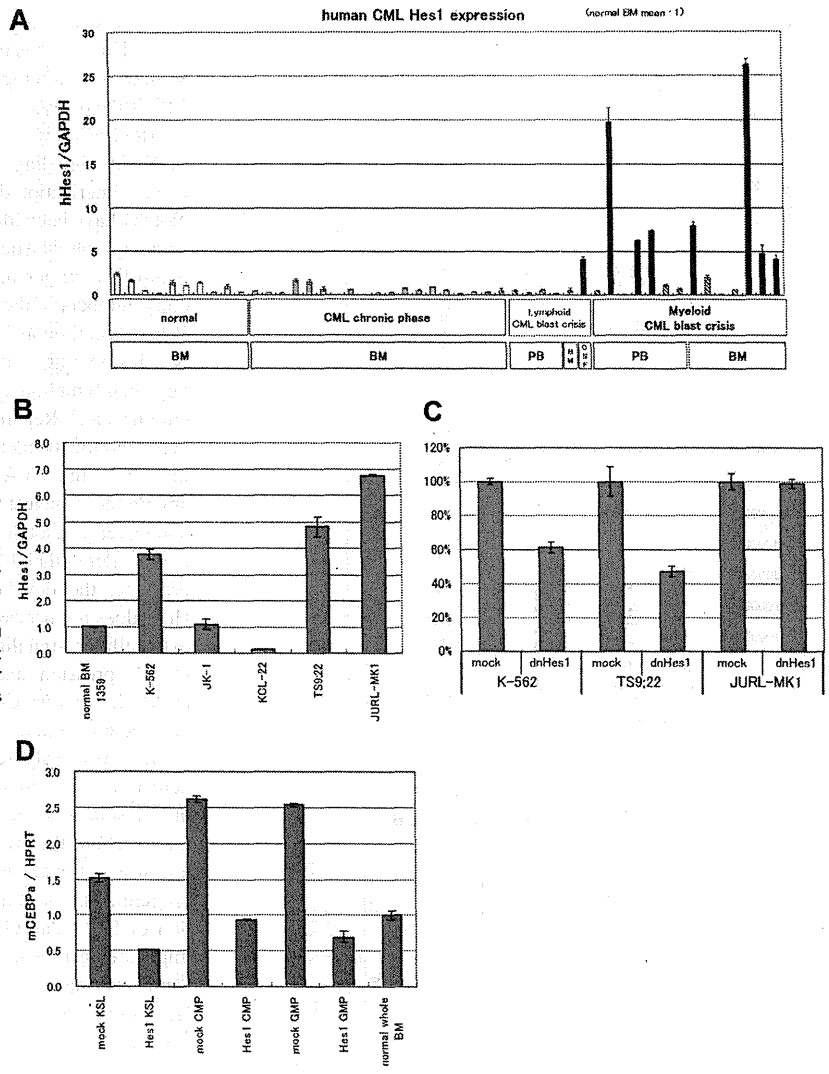

Figure 6. Hes1 expression was elevated in approximately 40% of patients with CML in blast crisis. (A) Real-time RT-PCR for Hes1 in bone marrow or peripheral blood cells from healthy subjects, patients with CML in chronic phase, or patients with CML in blast crisis. Expression levels were normalized by GAPDH mRNA. RNA from normal bone marrow cells served as a control (mean of 10 RNA levels of normal bone marrow was defined as 1). Hes1 mRNA levels exceeded 4 (solid bar) in 8 of 20 samples from CML in blast crisis patients. The correlation coefficient determined by the Wilcoxon signed-rank test between blast ratio and Hes1-expression level was −0.395. PB indicates peripheral blood; BM, bone marrow; CSF, cerebrospinal fluid. The solid bar represents CML in blast crisis exceeding 4; the hatched bar represents CML in blast crisis less than 4. (B) Hes1 expression in 5 human CML blast crisis cell lines. Expression levels of HES1 in K-562, JK-1, KCL-22, TS9:22, and JURL-MK1 were evaluated by real-time RT-PCR and were normalized by GAPDH mRNA. (C) Growth repression by transduction of dnHes1 (a dominant-negative Hes1) retrovirus vector into 3 human cell lines (K-562, TS9:22, and JURL-MK1). Six days after retrovirus transduction, cell numbers were counted. Growth is shown as a percentage of the control cells that were transduced with control vector. A representative result from 2 independent and reproducible experiments is shown. Error bars represent the SD from duplicate cultures. (D) Real-time RT-PCR for C/EBP-α in Hes1-transduced KSLs, CMPs, and GMPs compared with control vector-transduced KSLs, CMPs and GMPs. Total RNA was extracted at 60 hours from the initiation of Hes1-transduction. Error bars represent the SD from 2 independent experiments in (A-B,D).

in chronic phase patients. Although it is yet to be confirmed by a larger number of samples from CML as well as AML patients, this result indicates an interesting connection between the mouse model of AML/CML in blast crisis-like disease and human leukemia. In addition, we have demonstrated that transduction of dnHes1 represses the proliferation in 2 of 3 human cell lines of CML in blast crisis. These results suggest that Hes1 plays an important role in blast crisis of CML.

Although the origin of CML is considered to be a hematopoietic stem cell, blast crisis has been shown to be a result of transformation of myeloid progenitors.[16] BCR-ABL can cause MPN-like disease when introduced into the hematopoietic stem cell population but cannot induce MPN or leukemia when introduced into differentiated myeloid progenitors.[26] Therefore, development of full-blown AML/CML in blast crisis-like disease in mice with differentiated progenitors only by cotransduction with Hes1 and BCR-ABL may represent a true model of blast crisis of CML. In this context, Hes1 is a possible crisis-promoting gene like other examples, such as activated β-catenin[16] and BCL-2,[45] both of which caused CML in blast crisis-like disease in mice when transduced into GMPs together with BCR-ABL.

Several AML-associated fusion gene products, such as MLL-ENL,[46] MOZ-TIF2,[26] and MLL-AF9,[47] have been demonstrated to confer replating capacity on CMPs and GMPs, and eventually to transform these cells into leukemia-initiating cells. Unique to our findings is the fact that we transduced a wild-type transcription factor, Hes1, and found that such simple up-regulation of a transcription factor led to similar transformation phenotypes. A substantial number of examples have indicated that loss of function or altered function, rather than gain of function, of transcription factors, including MLL, MOZ, Runx1, RARα, C/EBP-α, etc, is associated with leukemogenesis. If up-regulation of Hes1 is indeed involved in human leukemias, this represents a new mechanism of leukemogenesis.

In modeling CML in mice, the present model provides a powerful tool by which we can induce 2 distinct phases of CML from stem cells or progenitors using BCR-ABL gene: a chronic phase-like state by transduction of KSL with BCR-ABL alone and a blast crisis-like state by cotransduction of CMPs and GMPs with BCR-ABL and Hes1.

In conclusion, we have developed a useful mouse model for CML blast crisis and have indicated that Hes1 is a key molecule in blast crisis transition in CML. The present mouse model will aid

Table 1. Clinical data of 20 patients with CML in blast crisis

Sample name	Source	Blast ratio	Hes1/GAPDH	Phenotype	Chromosome aberration	Clinical features
228 CML BC	PB	57	0.49	B-ALL	46,XY,t(9;22)/46,XY, +der(1;14)(q10;q12),t(9;22)	—
428 CML BC	PB	100	0.27	B-ALL	t(9;22)	—
984 CML BC	PB	60	0.56	B-ALL	46, XX, t(9;22)(q34;q11.2)	—
3259 CML BC	PB	100	0.16	B-ALL	t(9;22)	—
1385 CML BC	BM	81	0.56	B-ALL	t(9;22)	—
1107 CML BC	CSF	100	4.16	B-ALL	t(9;22)	The blasts increased drastically in CNS.
1 CML BC	PB	90	0.51	Myeloid	t(9;22)	—
219 CML BC	PB	12	19.72	Myeloid	45,XX,-7,t(9;22)	BM was dry tap composed of 100% blasts.
393 CML BC	PB	20	0.08	Myeloid	46,XX,t(9;22),add(17)(p11)	—
1088 CML BC	PB	30	6.22	Myeloid	46, XX, t(9;22)(q34;q11.2)	BM was dry tap.
1299 CML BC	PB	20	7.35	Myeloid	t(9;22)	BM was dry tap composed of 23% blasts.
1824 CML BC	PB	51	1.15	Myeloid	t(9;22)	BM was dry tap.
3153 CML BC	PB	7	0.66	Myeloid	t(9;22)	BM was dry tap. The blasts in BM increased up to 42% after taking this sample.
232 CML BC	BM	11	7.96	Myeloid	47,XY,+8,t(9;22)	The blasts in BM increased drastically up to 44% after taking this sample.
452 CML BC	BM	54	2.01	Myeloid	46,dic(17)(q10),t(9;22)	—
916 CML BC	BM	24	0.11	Myeloid	t(9;22)	—
1091 CML BC	BM	28	0.67	Myeloid	t(9;22)	—
811 CML BC	BM	25	26.25	Myeloid	46, XX, t(1;9;22)(q44;q34;q11.2)	—
3332 CML BC	BM	22	4.17	Myeloid	t(9;22)	—
3847 CML BC	BM	62	4.79	Myeloid	t(9;22)	—

CML indicates chronic myelogenous leukemia; BC, blast crisis; PB, peripheral blood; B-ALL, B-cell acute lymphoblastic leukemia; BM, bone marrow; CSF, cerebrospinal fluid; —, not applicable; and CNS, central nervous system.

understanding of the molecular mechanisms underlying blast crisis of CML and might lead to a better therapeutic outcome for this difficult disease.

Acknowledgments

The authors thank Dr R. Kageyama for the Hes1 cDNA; Dr H. Nakauchi and Dr M. Onodera for the GCDNsam/IRES-NGFR vector and the GCDNsam/IRES-GFP vector; Dr K. Akashi and Dr S. Mizuno for mouse C/EBP-α cDNA; Dr T. Inaba and Dr H. Asou (Hiroshima University, Hiroshima, Japan) for the JK-1, KCL-22, JURL-MK1 cell line; and Kirin Pharma for the TPO.

This work was supported by a Grant-in-Aid for Scientific Research (KAKENHI no. 20249051) and the Global Center of Excellence Program Center of Education and Research for the Advanced Genome-Based Medicine (for personalized medicine and the control of worldwide infectious diseases); the Ministry of Education, Culture, Sports, Science, and Technology of Japan (MEXT) and the Ministry of Health and Welfare of Japan (T.K.); and KAKENHI (no. 19390258), Astellas Foundation for Research on Metabolic Disorders, Uehara Memorial Foundation, and Princess Takamatsu Cancer Research Fund (S.C.).

Authorship

Contribution: F.N. did all the experiments and participated actively in writing the manuscript; M.S.-Y. and J.K. assisted with the experiments and actively participated in designing the experiments; Y.K., N.K., T.U., K.H., and K.K. assisted with the experiments; Y.H. and H.H. provided human samples; S.O. and M.K. participated in interpretation and designing the experiments; and T.K. and S.C. conceived the project, secured funding, and actively participated in manuscript writing.

Conflict-of-interest disclosure: T.K. serves as a consultant for R&D Systems and Rigel Pharmaceuticals. The remaining authors declare no competing financial interests.

Correspondence: Toshio Kitamura, Division of Stem Cell Signaling, Center for Stem Cell Therapy, Institute of Medical Science, University of Tokyo, 4-6-1 Shirokanedai, Minato-ku, Tokyo 108-8639, Japan; e-mail: kitamura@ims.u-tokyo.ac.jp; and Shigeru Chiba, Department of Hematology, Graduate School of Comprehensive Human Sciences, University of Tsukuba, 1-1-1 Tennodai, Tsukuba, Ibaraki 305-8575, Japan; e-mail: schiba-tky@umin.net.

References

1. Kageyama R, Nakanishi S. Helix-loop-helix factors in growth and differentiation of the vertebrate nervous system. *Curr Opin Genet Dev.* 1997;7(5):659-665.
2. Jarriault S, Brou C, Logeat F, Schroeter EH, Kopan R, Israel A. Signalling downstream of activated mammalian Notch. *Nature.* 1995;377(6547):355-358.
3. Jarriault S, Le Bail O, Hirsinger E, et al. Delta-1 activation of notch-1 signaling results in HES-1 transactivation. *Mol Cell Biol.* 1998;18(12):7423-7431.
4. Johnson JE, Birren SJ, Anderson DJ. Two rat homologues of Drosophila achaete-scute specifically expressed in neuronal precursors. *Nature.* 1990;346(6287):858-861.
5. Sumazaki R, Shiojiri N, Isoyama S, et al. Conversion of biliary system to pancreatic tissue in Hes1-deficient mice. *Nat Genet.* 2004;36(1):83-87.
6. Kumano K, Chiba S, Shimizu K, et al. Notch1 inhibits differentiation of hematopoietic cells by sustaining GATA-2 expression. *Blood.* 2001;98(12):3283-3289.
7. Kunisato A, Chiba S, Nakagami-Yamaguchi E, et al. HES-1 preserves purified hematopoietic stem cells ex vivo and accumulates side population cells in vivo. *Blood.* 2003;101(5):1777-1783.
8. Kaneta M, Osawa M, Sudo K, Nakauchi H, Farr AG, Takahama Y. A role for pref-1 and HES-1 in thymocyte development. *J Immunol.* 2000;164(1):256-264.
9. Tomita K, Hattori M, Nakamura E, Nakanishi S, Minato N, Kageyama R. The bHLH gene Hes1 is essential for expansion of early T cell precursors. *Genes Dev.* 1999;13(9):1203-1210.
10. Weng AP, Ferrando AA, Lee W, et al. Activating mutations of NOTCH1 in human T cell acute lymphoblastic leukemia. *Science.* 2004;306(5694):269-271.
11. Lee S-y, Kumano K, Nakazaki K, et al. Gain-of-function mutations and copy number increases of

Notch2 in diffuse large B-cell lymphoma. *Cancer Sci.* 2009;100(5):920-926.

12. Radtke F, Wilson A, Mancini SJ, MacDonald HR. Notch regulation of lymphocyte development and function. *Nat Immunol.* 2004;5(3):247-253.
13. Allman D, Punt JA, Izon DJ, Aster JC, Pear WS. An invitation to T and more: notch signaling in lymphopoiesis. *Cell.* 2002;109[suppl]:S1-S11.
14. Radtke F, Wilson A, Stark G, et al. Deficient T cell fate specification in mice with an induced inactivation of Notch1. *Immunity.* 1999;10(5):547-558.
15. Sakata-Yanagimoto M, Nakagami-Yamaguchi E, Saito T, et al. Coordinated regulation of transcription factors through Notch2 is an important mediator of mast cell fate. *Proc Natl Acad Sci U S A.* 2008;105(22):7839-7844.
16. Jamieson CH, Ailles LE, Dylla SJ, et al. Granulocyte-macrophage progenitors as candidate leukemic stem cells in blast-crisis CML. *N Engl J Med.* 2004; 351(7):657-667.
17. Akashi K, Traver D, Miyamoto T, Weissman IL. A clonogenic common myeloid progenitor that gives rise to all myeloid lineages. *Nature.* 2000; 404(6774):193-197.
18. Honda H, Fujii T, Takatoku M, et al. Expression of p210bcr/abl by metallothionein promoter induced T-cell leukemia in transgenic mice. *Blood.* 1995; 85(10):2853-2861.
19. Kitamura T, Koshino Y, Shibata F, et al. Retrovirus-mediated gene transfer and expression cloning: powerful tools in functional genomics. *Exp Hematol.* 2003;31(11):1007-1014.
20. Morita S, Kojima T, Kitamura T. Plat-E: an efficient and stable system for transient packaging of retroviruses. *Gene Ther.* 2000;7(12):1063-1066.
21. Sang L, Coller HA, Roberts JM. Control of the reversibility of cellular quiescence by the transcriptional repressor HES1. *Science.* 2008; 321(5892):1095-1100.
22. Hopfer O, Zwahlen D, Fey MF, Aebi S. The Notch pathway in ovarian carcinomas and adenomas. *Br J Cancer.* 2005;93(6):709-718.
23. Iwasaki H, Mizuno S, Mayfield R, et al. Identification of eosinophil lineage-committed progenitors in the murine bone marrow. *J Exp Med.* 2005; 201(12):1891-1897.
24. Ono R, Nakajima H, Ozaki K, et al. Dimerization of MLL fusion proteins and FLT3 activation synergize to induce multiple-lineage leukemogenesis. *J Clin Invest.* 2005;115(4):919-929.
25. Kawamata S, Du C, Li K, Lavau C. Overexpression of the Notch target genes Hes in vivo induces lymphoid and myeloid alterations. *Oncogene.* 2002;21(24):3855-3863.
26. Huntly BJ, Shigematsu H, Deguchi K, et al. MOZ-TIF2, but not BCR-ABL, confers properties of leukemic stem cells to committed murine hematopoietic progenitors. *Cancer Cell.* 2004;6(6):587-596.
27. Lozzio CB, Lozzio BB. Human chronic myelogenous leukemia cell-line with positive Philadelphia chromosome. *Blood.* 1975;45(3):321-334.
28. Okuno Y, Suzuki A, Ichiba S, et al. Establishment of an erythroid cell line (JK-1) that spontaneously differentiates to red cells. *Cancer.* 1990;66(7): 1544-1551.
29. Kubonishi I, Miyoshi I. Establishment of a Ph1 chromosome-positive cell line from chronic myelogenous leukemia in blast crisis. *Int J Cell Cloning.* 1983;1(2):105-117.
30. Gotoh A, Miyazawa K, Ohyashiki K, et al. Tyrosine phosphorylation and activation of focal adhesion kinase (p125FAK) by BCR-ABL oncoprotein. *Exp Hematol.* 1995;23(11):1153-1159.
31. Di Noto R, Luciano L, Lo Pardo C, et al. JURL-MK1 (c-kit(high)/CD30-/CD40-) and JURL-MK2 (c-kit(low)/CD30+/CD40+) cell lines: 'two-sided' model for investigating leukemic megakaryocytopoiesis. *Leukemia.* 1997;11(9):1554-1564.
32. Lee SY, Kumano K, Masuda S, et al. Mutations of the Notch1 gene in T-cell acute lymphoblastic leukemia: analysis in adults and children. *Leukemia.* 2005;19(10):1841-1843.
33. Allenspach EJ, Maillard I, Aster JC, Pear WS. Notch signaling in cancer. *Cancer Biol Ther.* 2002;1(5):466-476.
34. Fu L, Kogoshi H, Nara N, Tohda S. NOTCH1 mutations are rare in acute myeloid leukemia. *Leuk Lymphoma.* 2006;47(11):2400-2403.
35. Ingram WJ, McCue KI, Tran TH, Hallahan AR, Wainwright BJ. Sonic Hedgehog regulates Hes1 through a novel mechanism that is independent of canonical Notch pathway signalling. *Oncogene.* 2008;27(10):1489-1500.
36. Kamakura S, Oishi K, Yoshimatsu T, Nakafuku M, Masuyama N, Gotoh Y. Hes binding to STAT3 mediates crosstalk between Notch and JAK-STAT signalling. *Nat Cell Biol.* 2004;6(6):547-554.
37. Nerlov C. C/EBPalpha mutations in acute myeloid leukaemias. *Nat Rev Cancer.* 2004;4(5):394-400.
38. Gombart AF, Hofmann WK, Kawano S, et al. Mutations in the gene encoding the transcription factor CCAAT/enhancer binding protein alpha in myelodysplastic syndromes and acute myeloid leukemias. *Blood.* 2002;99(4):1332-1340.
39. Smith ML, Cavenagh JD, Lister TA, Fitzgibbon J. Mutation of CEBPA in familial acute myeloid leukemia. *N Engl J Med.* 2004;351(23):2403-2407.
40. Zhang P, Iwasaki-Arai J, Iwasaki H, et al. Enhancement of hematopoietic stem cell repopulating capacity and self-renewal in the absence of the transcription factor C/EBP alpha. *Immunity.* 2004;21(6):853-863.
41. Koschmieder S, Halmos B, Levantini E, Tenen DG. Dysregulation of the C/EBPalpha differentiation pathway in human cancer. *J Clin Oncol.* 2009;27(4):619-628.
42. Kirstetter P, Schuster MB, Bereshchenko O, et al. Modeling of C/EBPalpha mutant acute myeloid leukemia reveals a common expression signature of committed myeloid leukemia-initiating cells. *Cancer Cell.* 2008;13(4):299-310.
43. Fan X, Mikolaenko I, Elhassan I, et al. Notch1 and notch2 have opposite effects on embryonal brain tumor growth. *Cancer Res.* 2004;64(21): 7787-7793.
44. Hallahan AR, Pritchard JI, Hansen S, et al. The SmoA1 mouse model reveals that notch signaling is critical for the growth and survival of sonic hedgehog-induced medulloblastomas. *Cancer Res.* 2004;64(21):7794-7800.
45. Jaiswal S, Traver D, Miyamoto T, Akashi K, Lagasse E, Weissman IL. Expression of BCR/ABL and BCL-2 in myeloid progenitors leads to myeloid leukemias. *Proc Natl Acad Sci U S A.* 2003;100(17):10002-10007.
46. Cozzio A, Passegue E, Ayton PM, Karsunky H, Cleary ML, Weissman IL. Similar MLL-associated leukemias arising from self-renewing stem cells and short-lived myeloid progenitors. *Genes Dev.* 2003;17(24):3029-3035.
47. Krivtsov AV, Twomey D, Feng Z, et al. Transformation from committed progenitor to leukaemia stem cell initiated by MLL-AF9. *Nature.* 2006;442(7104): 818-822.

Leukemia (2010) 24, 1018–1024

www.nature.com/leu

ORIGINAL ARTICLE

AID-induced T-lymphoma or B-leukemia/lymphoma in a mouse BMT model

Y Komeno[1,2], J Kitaura[1,2], N Watanabe-Okochi[3,4], N Kato[1,2], T Oki[1,2], F Nakahara[1,2], Y Harada[5], H Harada[6], R Shinkura[7], H Nagaoka[7], Y Hayashi[8], T Honjo[7] and T Kitamura[1,2]

[1]Division of Cellular Therapy, Advanced Clinical Research Center, Institute of Medical Science, University of Tokyo, Minato-ku, Tokyo, Japan; [2]Division of Stem Cell Signaling, Center for Stem Cell Therapy, Institute of Medical Science, University of Tokyo, Minato-ku, Tokyo, Japan; [3]Department of Hematology and Oncology, Graduate School of Medicine, University of Tokyo, Bunkyo-ku, Tokyo, Japan; [4]Department of Transfusion Medicine, Graduate School of Medicine, University of Tokyo, Bunkyo-ku, Tokyo, Japan; [5]International Radiation Information Center, Research Institute for Radiation Biology and Medicine, Hiroshima University, Minami-ku, Hiroshima, Japan; [6]Department of Hematology and Oncology, Research Institute for Radiation Biology and Medicine, Hiroshima University, Minami-ku, Hiroshima, Japan; [7]Department of Immunology and Genomic Medicine, Graduate School of Medicine, Kyoto University, Sakyo-ku, Kyoto, Japan and [8]Department of Hematology/Oncology, Gunma Children's Medical Center, Shibukawa, Gunma, Japan

Activation-induced cytidine deaminase (AID) diversifies immunoglobulin through somatic hypermutation (SHM) and class-switch recombination (CSR). AID-transgenic mice develop T-lymphoma, indicating that constitutive expression of AID leads to tumorigenesis. Here, we transplanted mouse bone marrow cells transduced with AID. Twenty-four of the 32 recipient mice developed T-lymphoma 2–4 months after the transplantation. Surprisingly, unlike AID-transgenic mice, seven recipients developed B-leukemia/lymphoma with longer latencies. None of the mice suffered from myeloid leukemia. When we used nude mice as recipients, they developed only B-leukemia/lymphoma, presumably due to lack of thymus. Analysis of AID mutants suggested that an intact form with SHM activity is required for maximum ability of AID to induce lymphoma. Except for a K-ras active mutant in one case, specific mutations could not be identified in T-lymphoma; however, Notch1 was constitutively activated in most cases. Importantly, truncations of Ebf1 or Pax5 were observed in B-leukemia/lymphoma. In conclusion, this is the first report on the potential of AID overexpression to promote B-cell lymphomagenesis in a mouse model. Aberrant expression of AID in bone marrow cells induced leukemia/lymphoma in a cell-lineage–dependent manner, mainly through its function as a mutator.
Leukemia (2010) **24,** 1018–1024; doi:10.1038/leu.2010.40;
published online 1 April 2010
Keywords: AID; BMT; T-lymphoma; B-leukemia/lymphoma

Introduction

Under physiological conditions, activation-induced cytidine deaminase (AID) is expressed in germinal center (GC) B-cells and initiates somatic hypermutation (SHM) and class-switch recombination (CSR) by deaminating a cytosine to create a uracil.[1,2] Structurally, the N-terminal or C-terminal domain of AID is indispensable for SHM or CSR, respectively.[3–5] Interestingly, expression of AID is increased in B-lymphoid leukemia or GC-derived B-lymphoma, with frequent hypermutation of proto-oncogenes and reciprocal chromosomal translocation.[6–9] In fact, recent studies have shown that AID is required for GC-derived lymphomagenesis and c-Myc/IgH chromosomal translocations.[10,11] In addition, elevated expression of endogenous AID and aberrant somatic mutations in tumor-related genes have also been observed in cancerous tissues related to inflammation.[12] Analysis of AID-transgenic (Tg) mice has revealed that constitutive expression of AID leads to tumorigenesis; ubiquitous and constitutive expression of AID induced lethal T-lymphoma with no apparent chromosomal translocation, occasionally accompanied by lung, liver, and gastric cancers,[13,14] and specific expression of AID in double-positive thymocytes also induced T-lymphoma.[15] However, neither AID-Tg mice specifically expressing AID in single-positive thymocytes and mature T-cells nor AID-Tg mice with $CD19^+$ B-cell-specific expression of AID developed lymphoma/leukemia.[15,16] These results suggest that susceptibility to AID-induced tumorigenesis depends on tissue or cell lineage, but the underlying mechanism remains obscure. Importantly, sequencing analysis in AID-Tg mice indicated that AID is an organ-specific mutator of non-Ig genes.[14] To prevent accumulation of unfavorable mutations induced by AID, its activity is tightly regulated by several mechanisms.[17]

In this study, we focused on AID-mediated leukemogenesis and created a mouse bone marrow transplantation (BMT) model, using BM cells retrovirally transduced with AID. Notably, recipient mice developed B-leukemia/lymphoma, albeit less frequently as compared with thymic T-lymphoma.

Materials and methods

Retroviral constructs, transfection, and retrovirus production

Murine AID (mAID), mAID mutants ($G23S^4$ and $\Delta189–198^5$), human AID (hAID), and hAID mutants ($P20^3$ and $JP8B^3$) were subcloned into the pMYsIG vector as described in 'Supplementary Materials and methods'. All constructs were verified by DNA sequencing. Expression of wild-type or mutant AID was recognized in 293T cells transiently transfected with each construct. Retroviruses were generated by transient transfection of Plat-E packaging cells with FuGene 6 (Roche Diagnostics, Mannheim, Germany), as described earlier.[18–20]

Mouse BMT

Mouse BMT was performed as described earlier.[20] C57BL/6 CD45.1 or CD45.2 mice were used as donors or recipients,

Correspondence: Dr T Kitamura, Division of Cellular Therapy, Advanced Clinical Research Center, Institute of Medical Science, University of Tokyo, 4-6-1 Shirokanedai, Minato-ku, Tokyo 108-8639, Japan.
E-mail: kitamura@ims.u-tokyo.ac.jp
Received 23 November 2009; revised 8 January 2010; accepted 9 February 2010; published online 1 April 2010

respectively. Infected cells (2×10^5) were intravenously injected into recipient mice, which had been administered a sublethal dose of γ-irradiation. Overall survival was estimated using the Kaplan–Meier method and log-rank test. Data are presented as the means ± s.d. PB smears and cytospin slides were stained with Hemacolor (Merck, Darmstadt, Germany). Tissues were fixed in 4% w/v buffered formalin, embedded in paraffin, and then sliced and stained with standard hematoxylin and eosin. All animal studies were approved by the Animal Care Committee of the Institute of Medical Science, The University of Tokyo.

Flow cytometric analysis

Cells were stained with phycoerythrin-conjugated monoclonal antibodies (eBiosciences, San Diego, CA, USA), as described.[20] Flow cytometric analysis was performed with a FACSCalibur equipped with CellQuest software (BD Biosciences, San Jose, CA, USA) and Flowjo software (Tree Star, San Carlos, CA, USA).

Western blotting

Equal numbers of cells were denatured in pre-heated sample buffer. Western blotting was performed as described.[20] Anti-AID mAb raised against the N-terminus of mAID, and anti-α-tubulin Ab (T6074, Sigma-Aldrich, St Louis, MO, USA) were used.

Southern blotting

Southern blotting was performed as described.[20] Briefly, 10 μg of genomic DNA digested with *EcoRI* was electrophoresed on a 0.7% agarose gel. Proviruses were probed with a ^{32}P-labeled GFP probe.

Reverse transcription and real-time PCR

Real-time PCR was performed using LightCycler (Roche Diagnostics), as described.[20] cDNA was amplified using a SYBR Premix EX Taq (Takara, Shiga, Japan). Primer pairs and conditions used for real-time PCR are listed in 'Supplementary Materials and methods'. Informed consent for the use of the human leukemia/lymphoma cells was obtained from patients in accordance with the Declaration of Helsinki, and study approval was obtained from the ethics committee of the Institute of Medical Science, the University of Tokyo (Approval Number 20-10-0620).

Sequencing of target genes

Genomic PCR was performed by using AmpliTaq Gold (Roche Molecular Systems Inc., Branchburg, NJ, USA) and the primer pairs described in 'Supplementary Materials and methods'. The PCR products were gel-purified and directly sequenced. If necessary, PCR products were subcloned and sequenced.

Treatment of AID-induced T-lymphoma cell lines with γ-secretase inhibitor

Cell lines of AID-induced T-lymphoma were established by culturing tumor cells in RPMI1640 with 20% FBS. Human T-acute lymphoblastic leukemia (T-ALL) cell lines Jurkat and HPB-ALL were cultured in RPMI1640 with 10% FBS. Various concentrations of γ-secretase inhibitor (DAPT, 565770, Calbiochem, Darmstadt, Germany) or vehicle (DMSO, Wako, Osaka, Japan) were added to 5×10^3 cells for 72 h. Cell growth was estimated by using CellTiter-Glo (Promega, Madison, WI, USA). Cleavage of intracellular domains of Notch1 (ICN) was detected by anti-ICN antibody (2421, Cell Signaling, Beverly, MA, USA) in western blotting.

Results

Transduction with AID into BM cells causes B-leukemia/lymphoma as well as thymic T-lymphoma in a mouse BMT model

First, we asked whether transduction of wild-type mAID (WT) into BM cells caused leukemia/lymphoma other than T-lymphoma in a BMT model ($n=32$) (Figure 1). We confirmed efficient retrovirus infection: 50–70% and 76–84% of the BM cells transduced with WT or mock, respectively, were GFP-positive before transplantation. The recipient mice of WT-transduced cells developed thymic T-lymphoma more frequently than did AID-Tg mice[13] (75 vs 35%). The disease was associated with hepatosplenomegaly, killing the mice in 2–4 months after transplantation (Figure 1a; Supplementary Figure 1; Supplementary Table 1). Histological and flow cytometric analyses showed that the thymus was filled with the T-lymphoblastic cells $CD3^{dull}$, $CD4^+$, $CD8^+$, and $Thy1.2^+$, indicating the differentiation block at early stages of T-cell development in thymus (Figures 1b–d). The complete blood counts of these mice were usually normal, except for the increase of T-lymphoblastic cells or mature granulocytes in some cases (Supplementary Figure 1; Supplementary Table 1, and data not shown). Notably, 7 of 32 transplanted mice (22%) developed B-leukemia/lymphoma with pancytopenia and splenomegaly, and died with significantly longer latencies as compared with those of T-lymphoma (Figures 1a–d; Supplementary Figure 1; Supplementary Table 1). Spleen and BM were filled with B-lymphoblastic cells in most cases, while affected lymph nodes differed in size among cases. B-lymphoma cells were $B220^+$, $CD19^+$, $CD43^{dull/+}$, $c\text{-}kit^{dull/+}$, and IgM^- (Figure 1d). Neither Bcl-6 induction[21,22] nor abnormal Ikaros deletions[23] were detected in these cells (data not shown). There was a wide range of GFP-positive ratios among AID-induced T- or B-lymphoma cells, irrespective of disease severity (Supplementary Figure 2 and data not shown). Sequencing analysis of GFP gene integrated into the genome revealed multiple mutations, resulting in reduced green fluorescence. Interestingly, one recipient developed both T- and B-lymphoma. None of the mice suffered from myeloid leukemia. The lymphoma cells, irrespective of T- or B-lineage, were serially transplantable and developed T- or B-leukemia with shorter latencies, respectively (data not shown). The recipient mice of mock-transduced cells did not develop any leukemia/lymphoma (Figure 1a). Collectively, transduction with AID into BM cells led to thymic T-lymphoma or B-leukemia/lymphoma, but not myeloid leukemia in a mouse BMT model. Similar results were obtained when Balb/c mice were used (data not shown).

We next asked whether the integration of retroviruses influenced the different phenotypes (T- or B-lymphoma) in AID-induced leukemogenesis. Southern blot analysis demonstrated a single or several proviral integrations in T-lymphoma samples (Figure 1e, left panel). On the other hand, we found that a single integration was predominant in B-lymphoma samples (Figure 1e, right panel). In one recipient harboring both T- and B-lymphoma, a distinct integration was confirmed in each sample (Figure 1e, right panel, lanes *B and *T), indicating the double cancer in this case. We identified a single or several retroviral integration sites (RIS) from lymphoma samples by inverse PCR method (Supplementary Table 2). However, we could not find any specific relationship between RIS and different phenotypes of lymphomas. In addition, a common integration site was identified only in one recipient (ID69) (Supplementary Table 2). These results suggested that AID-induced lymphomagenesis mainly depended on its intrinsic function, but not RIS.

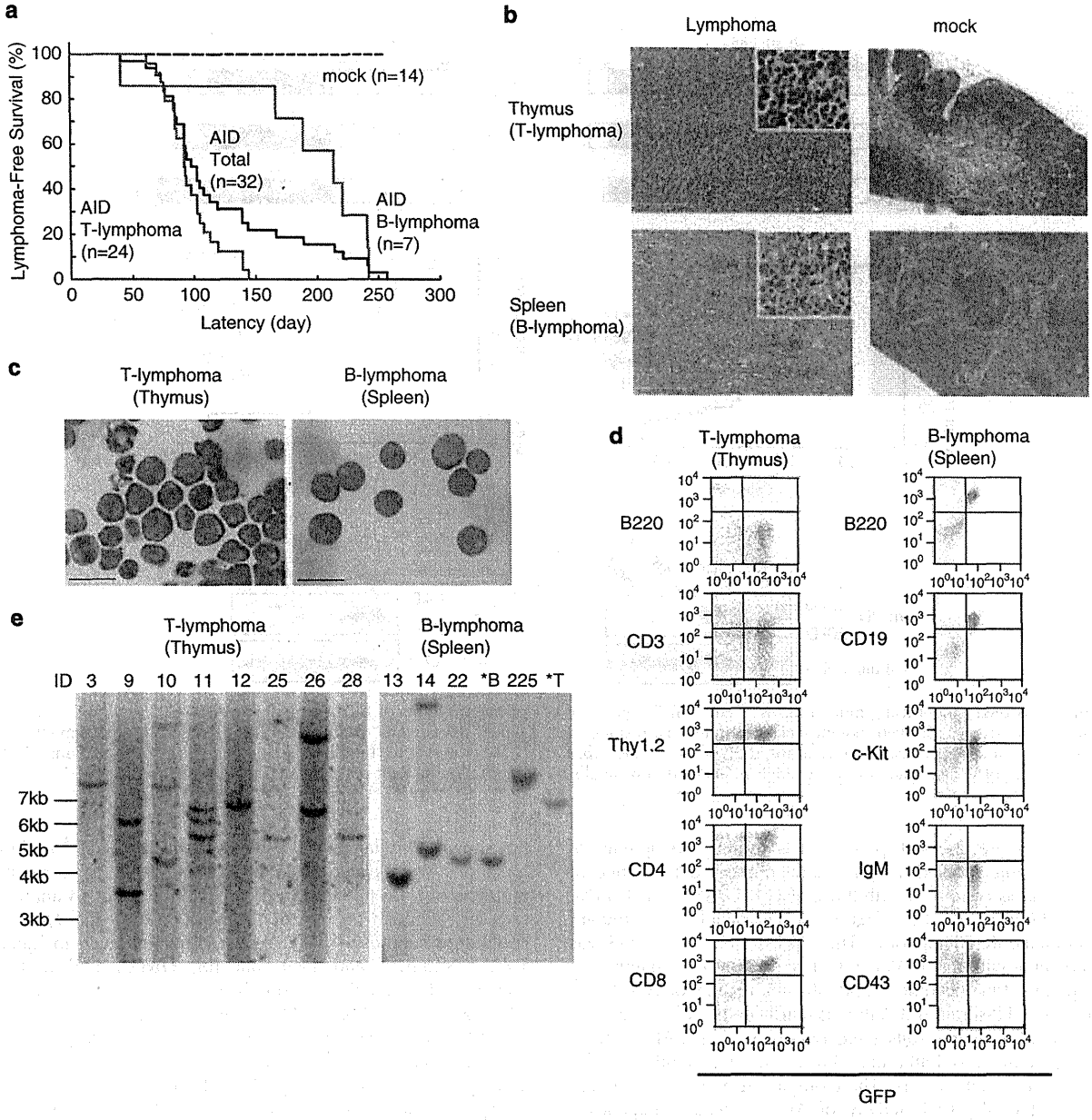

Figure 1 AID-induced T-lymphoma and B-leukemia/lymphoma in a mouse BMT model. (**a**) Kaplan–Meier plot of survival (black lines). Survival curve for AID recipient mice that developed T-lymphoma or B-lymphoma is indicated by green or red line, respectively. (**b**) Hematoxylin and eosin staining of AID-induced T-lymphoma (thymus, upper/left panel), control thymus (upper/right panel), AID-induced B-lymphoma (spleen, lower/left panel), or control spleen (lower/right panel). Magnifications × 200 (overview) and × 400 (insert). Scale bars: 200 μm. (**c**) Cytospin preparations of T-lymphoma (left panel) and B-lymphoma (right panel). Magnification × 1000. Scale bars: 20 μm. (**d**) Flow cytometric analysis of lymphoma cells. (**e**) Southern blotting of T-lymphoma (left panel) and B-lymphoma (right panel). *B or *T in the right panel indicates B- or T-lymphoma, respectively, which was found in the same mouse (ID 29).

We then asked whether other hematopietic malignancies, including myeloid leukemia, are induced in the absence of thymus. We used athymic nude mice as recipients of a BMT model, finding that 5 of 8 nude mice transplanted with AID-transduced BM cells developed B-leukemia/lymphoma, but no other hematopoietic diseases were observed (Supplementary Figure 3). Thus, B-leukemia/lymphoma was predominantly induced in the absence of thymus, but transduction of AID into BM cells did not induce myeloid leukemia. Altogether, these results suggested that the oncogenic transformation of AID-transduced BM cells requires *in vivo* environment suitable for differentiation and proliferation of immature lymphoid cells.

Impaired lymphomagenesis by SHM-defective AID mutants

To examine how SHM and/or CSR activities of AID contribute to lymphomagenesis, we constructed a BMT model using mutant forms of AID: missense mutant G23S with decreased SHM activity[4]; and truncation mutant Δ189–198 defective for CSR

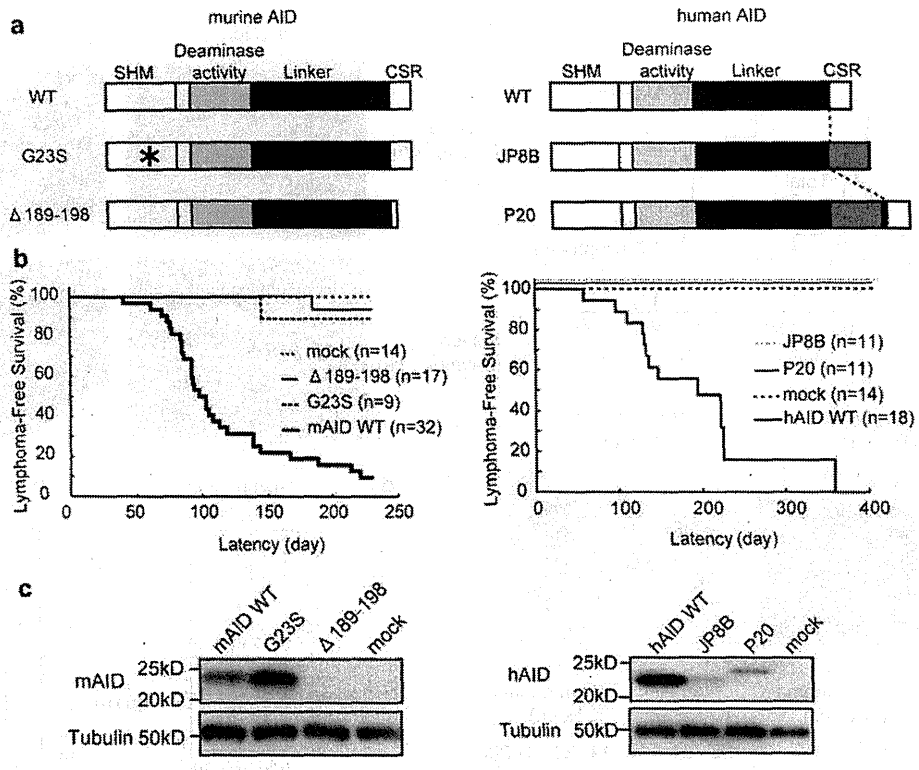

Figure 2 A BMT model using mutant forms of AID. (**a**) Diagrams of WT or mutant forms of AID. Left panel, mAID. G23S harbors a missense mutation (asterisk). Δ189–198 mutant lacks C-terminal 10 residues. Right panel, human AID (hAID). JP8B has a frameshift replacement of the C-terminus with 26 residues. P20 has an insertion of 34 residues. (**b**) Kaplan–Meier curves for the survival. Left panel, mAID. Right panel, hAID. (**c**) Expression of WT or mutant forms of AID in GFP-sorted BM cells by western blotting. Left panel, mAID. Right panel, hAID.

activity (Figure 2a, left panel).[5] Interestingly, recipients of these mutants showed a significantly decreased incidence of lymphoma as compared with those of WT (G23S $n=1/9$, 11%; Δ189–198 $n=1/17$, 6%) (Figure 2b, left panel). Each mutant developed only T-lymphoma. The expression level of G23S was comparable with that of WT in GFP-sorted BM cells (Figure 2c, left panel). On the other hand, the expression of Δ189–198 mutant in GFP-sorted BM cells was hardly detectable (Figure 2c, left panel). Similar results were obtained when hAID and its C-terminal mutants JP8B and P20 were transduced into BM cells (Figures 2a–c, right panels). Therefore, it was difficult to evaluate the effect of the CSR activity of AID on lymphomagenesis. Altogether, these results suggest that the intact form of AID with SHM activity is required to maximally exert its oncogenic activity.

An active mutation of K-ras in one case as well as multiple point mutations of Notch1, PTEN, and c-Myc was observed in AID-induced T-lymphoma

As point mutations are introduced into non-Ig genes such as *TCR* or *c-Myc* gene in T-lymphoma cells of AID-Tg mice,[13] we next asked which mutations caused by AID were responsible for T-lymphomagenesis in a mouse BMT model. On the basis of the fact that AID-mediated mutations occur after about 100 nucleotides downstream of the promoter and extend to 1–2 kb,[24] we performed genomic sequencing of several possible target genes in the region encompassing 0.5–1 kb from the transcription start site, in addition to the mutational hotspots implicated in tumorigenesis (Supplementary Table 3 and data not shown). Similar to the results on AID-Tg mice,[13] multiple mutations were observed in the *c-Myc* gene. An activating mutation of *K-ras* (G13D) was detected in 1 out of 14 analyzed samples, although no mutation was found in *N-ras*, *H-ras*, or *p53* tumor suppressor gene. As for genes involved in human T-ALL, *Notch1*[25] and *Pten*, but not *Fbxw7*, had multiple mutations. Intriguingly, we found several mutations in exon 27 (HD domain) and exon 34 (PEST domain), mutational hotspots of *Notch1* far downstream from the transcription start site. Consistent with the earlier report,[13] detected mutations were predominantly transition mutations and strongly biased to GC bases. Collectively, multiple mutations in T-lymphoma were introduced by AID, probably in association with lymphomagenesis.

Most AID-induced T-lymphoma cells exhibited constitutive activation of Notch1 and were susceptible to a γ-secretase inhibitor

The finding that Notch1 mutations were observed in AID-induced T-lymphoma led us to address the question of whether these mutations caused the activation of Notch1, leading to T-lymphomagenesis. Interestingly, western blot analysis demonstrated that cleavage of intracellular Notch1 (ICN) was evident in most T-lymphoma samples tested (Figure 3a), indicating that constitutive activation of Notch1 occurred in most T-lymphoma cells. In support of this finding, real-time PCR analysis showed increased expression of Hes1 and c-Myc and decreased expression of PTEN in most samples (Figure 3b). Expression levels of Notch1 did not significantly vary among these samples, except for a few cases. Interestingly, when we treated two cell

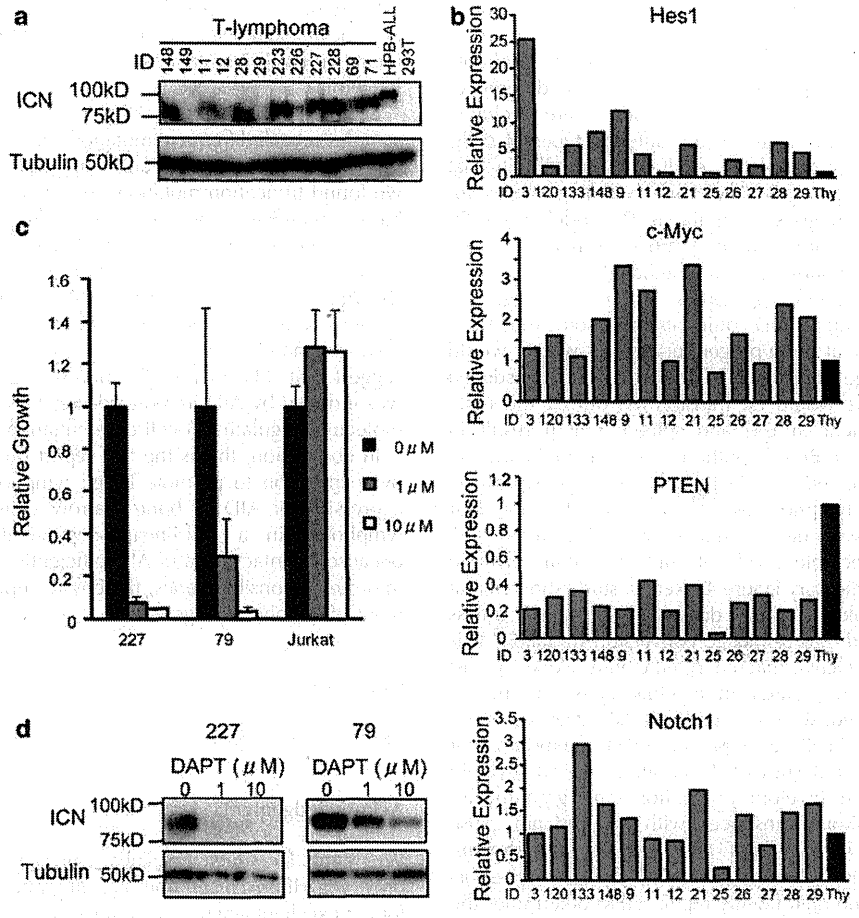

Figure 3 Notch1 is constitutively activated in AID-induced T-lymphoma. (**a**) Cleavage of intracellular Notch1 (ICN) in AID-induced T-lymphoma confirmed by western blotting. (**b**) Relative expression levels of Hes1, c-Myc, PTEN, or Notch1 in T-lymphoma samples and normal thymocytes (Thy) measured by real-time PCR. (**c**) The relative growth estimated by colorimetric assay. Two cell lines 227 and 79 established from AID-induced T-lymphoma, or Jurkat cells were treated with indicated concentrations of DAPT for 72 h. The means ± s.d. of triplicate measurements are shown. Data are representative of three independent experiments. (**d**) Cleavage of ICN examined by western blotting. Cells were treated as described in (**c**). Data are representative of three independent experiments.

lines established from AID-induced T-lymphoma with a γ-secretase inhibitor, DAPT, the growth as well as the cleavage of ICN of these cell lines was dose dependently inhibited by DAPT (Figures 3c and d). Although Notch1 mutations did not account for constitutive activation of Notch1 in all cases, these results indicated that T-lymphomagenesis in most cases was induced by Notch1 activation, probably in conjunction with AID-introduced mutations of the related genes.

Truncation mutations of Ebf1 and Pax5 were found in AID-induced B-lymphoma

To investigate the relevant mechanism of AID-induced B-lymphomagenesis, we performed genomic sequencing of the *Ebf1* and *Pax5* genes of AID-induced B-leukemia/lymphoma of seven recipient mice (Supplementary Table 4 and data not shown). Intriguingly, sequencing of *Ebf1* revealed a 23-base deletion and a 4-base insertion in exon 2, which together resulted in truncation in one sample. In addition, multiple point mutations were found in three samples. As for *Pax5*, we found a truncation caused by a couple of 2-base deletions and a point mutation in exon 1a in one case, and point mutations in two cases. On the basis of the recent study,[26] the aberrations of *Pax5* and *Ebf1* genes described above might have some function in B-lymphomagenesis in the recipient mice. On the other hand, we did not find c-Myc/IgH chromosomal translocations in B-lymphoma samples analyzed by PCR combined with Southern blotting (data not shown).[27] Collectively, these results suggested that B-lymphomagenesis in a BMT model was, at least in part, due to AID-introduced mutations/deletions of the genes regulating B-cell differentiation.

Discussion

In this study, we constructed a mouse BMT model to test whether AID is implicated in the pathogenesis of leukemia/lymphoma including myeloid leukemia. Our results revealed that aberrant expression of AID in BM cells led to T-lymphoma and less frequently B-leukemia/lymphoma, but not myeloid leukemia (Figure 1). The recipient mice developed 'thymic' T-lymphoma, but not 'peripheral type' T-lymphoma observed in 65% of AID-Tg mice.[13] It was noteworthy that B-leukemia/lymphoma was observed in our BMT model, but not in AID-Tg

mice,[13,15,28] because AID is implicated in the pathogenesis of human B-cell malignancy.[6–9] Interestingly, nude mice developed only B-leukemia when used as recipients, probably due to lack of thymus (Supplementary Figure 3). The differences between AID-Tg mice and the BMT model were probably caused by the expression levels in the different types of cells, although we could not completely exclude the possibility that RIS affected the phenotypes. We have two hypotheses for AID-induced lymphomagenesis in the BMT model: (1) AID-transduced stem/progenitor cells may move to thymus, where they would be susceptible to AID-mediated mutations and rapidly acquire oncogenic properties at an early stage of T-lineage development; (2) AID could introduce some mutations and transform cells at stem/progenitor levels, which would commit to T-lineage in thymus. Otherwise, AID-transduced stem/progenitor cells would be transformed during the early B-lineage development in BM and spleen, which result in B-leukemia/lymphoma. Both hypotheses would explain why no lymphoma was observed in AID-Tg mice with its expression restricted to mature lymphocytes.[15,28] However, it is not clear why AID overexpression did not induce myeloid leukemia. We found scarcely detectable levels of AID in human myeloid malignancy (Supplementary Figure 4). Recent study showed that chronic myeloid leukemia (CML) does not express AID unless CML cells are forced into B-lineage conversion by Pax5.[9] It is possible that the protective machinery efficiently works against AID functioning as a mutator in myeloid cells, but not in lymphoid cells. Indeed, we confirmed that AID overexpression did not affect myeloid cell development in BM one month after transplantation (data not shown). In addition, sorted myeloid progenitors (common myeloid progenitors and granulocyte-macrophage progenitors) transduced with AID did not cause myeloid leukemia in our BMT model (data not shown). According to the recent studies, the balance between error-prone repair (EPR) and high-fidelity repair (HFR) determines the outcome of AID-generated uracils, that is, accumulation or elimination of mutations.[29] It is tempting to speculate that the frequencies of uracils generated by AID are not different between the myeloid- and lymphoid-lineage, but that HFR overcomes EPR in the myeloid-lineage. In any case, solving the riddle of how AID induces leukemia/lymphoma in a cell-lineage–dependent manner will help understand AID functions.

It is generally accepted that the N-terminal or C-terminal domain of AID is important for SHM or CSR activity, respectively,[3–5] but neither activity is regulated in an exclusively distinct way. Our results showed that AID mutants with decreased SHM or CSR activity have impaired oncogenic activity (Figure 2). It must be noted that expression levels of mouse mutant Δ189–198 as well as human mutants JP8B and P20 in GFP-sorted BM cells were lower than those of WTs, possibly due to protein instability of these C-terminal mutants.[30] Therefore, we cannot answer the question whether CSR activity is indispensable for oncogenicity of AID, but we assume that the maximum ability of AID to cause lymphoma requires an intact form of AID with SHM activity.

We clarified to some extent the mechanism by which AID-introduced mutations of tumor-related genes led to lymphomagenesis (Supplementary Table 3). As reported on AID-Tg mice,[13] multiple mutations of the *c-Myc* gene were found in T-lymphoma samples. The *Notch1* gene was mutated in exon 1 and mutational hotspots (HD and PEST domains) in four cases. Intriguingly, Notch1 was constitutively activated in T-lymphoma more frequently than expected from the mutation frequency of *Notch1* (Figure 3). We speculate that AID-mediated mutations of other genes caused secondary Notch1 activation, resulting in T-lymphoma. However, one such candidate, *Fbxw7*,[31] did not have significant mutations. Further examination will identify unknown mutations responsible for human T-lymphoma/leukemia.

Sequencing analysis of AID-induced B-leukemia/lymphoma samples revealed frequent mutations in the *Ebf1* and *Pax5* genes (Supplementary Table 4 and data not shown). Importantly, we found truncation mutations in *Ebf1* and *Pax5* that probably have oncogenic properties; mono-allelic deletions of these genes were observed in human B-ALL.[26] As for chromosomal instability, c-Myc/IgH translocation was not detected (data not shown). The presence of TCR translocations was unlikely, as no chromosomal translocation was detected in AID-induced T-lymphoma observed in AID-Tg mice.[13,15] The present results suggest that, like thymic T-lymphoma, B-leukemia/lymphoma was induced by AID-introduced mutations/deletions of the key molecules regulating B-cell differentiation and/or proliferation.

In conclusion, this is the first report on the potential of AID overexpression to promote B-cell lymphomagenesis. Aberrant expression of AID in bone marrow cells induced leukemia/lymphoma in a cell-lineage–dependent manner, probably because an intact form of AID efficiently introduced mutations into the responsible genes, thereby disrupting normal development of lymphoid progenitors.

Conflict of interest

TK serves as a consultant for R&D Systems.

Acknowledgements

We thank Dr Chiba (Tsukuba University, Ibaraki, Japan) for providing HPB-ALL cell line. We are grateful to Dr Dovie Wylie for her excellent language assistance. This work was supported by grants from the Ministry of Education, Science, Technology, Sports and Culture, Japan to TK.

References

1 Muramatsu M, Sankaranand VS, Anant S, Sugai M, Kinoshita K, Davidson NO *et al.* Specific expression of activation-induced cytidine deaminase (AID), a novel member of the RNA-editing deaminase family in germinal center B cells. *J Biol Chem* 1999; **274**: 18470–18476.
2 Muramatsu M, Kinoshita K, Fagarasan S, Yamada S, Shinkai Y, Honjo T. Class switch recombination and hypermutation require activation-induced cytidine deaminase (AID), a potential RNA editing enzyme. *Cell* 2000; **102**: 553–563.
3 Ta VT, Nagaoka H, Catalan N, Durandy A, Fischer A, Imai K *et al.* AID mutant analyses indicate requirement for class-switch-specific cofactors. *Nat Immunol* 2003; **4**: 843–848.
4 Shinkura R, Ito S, Begum NA, Nagaoka H, Muramatsu M, Kinoshita K *et al.* Separate domains of AID are required for somatic hypermutation and class-switch recombination. *Nat Immunol* 2004; **5**: 707–712.
5 Barreto V, Reina-San-Martin B, Ramiro AR, McBride KM, Nussenzweig MC. C-terminal deletion of AID uncouples class switch recombination from somatic hypermutation and gene conversion. *Mol Cell* 2003; **12**: 501–508.
6 Pasqualucci L, Neumeister P, Goossens T, Nanjangud G, Chaganti RS, Kuppers R *et al.* Hypermutation of multiple proto-oncogenes in B-cell diffuse large-cell lymphomas. *Nature* 2001; **412**: 341–346.
7 Greeve J, Philipsen A, Krause K, Klapper W, Heidorn K, Castle BE *et al.* Expression of activation-induced cytidine deaminase in human B-cell non-Hodgkin lymphomas. *Blood* 2003; **101**: 3574–3580.

8 Smit LA, Bende RJ, Aten J, Guikema JE, Aarts WM, van Noesel CJ. Expression of activation-induced cytidine deaminase is confined to B-cell non-Hodgkin's lymphomas of germinal-center phenotype. *Cancer Res* 2003; **63**: 3894–3898.
9 Klemm L, Duy C, Iacobucci I, Kuchen S, von Levetzow G, Feldhahn N *et al.* The B cell mutator AID promotes B lymphoid blast crisis and drug resistance in chronic myeloid leukemia. *Cancer Cell* 2009; **16**: 232–245.
10 Pasqualucci L, Bhagat G, Jankovic M, Compagno M, Smith P, Muramatsu M *et al.* AID is required for germinal center-derived lymphomagenesis. *Nat Genet* 2008; **40**: 108–112.
11 Takizawa M, Tolarova H, Li Z, Dubois W, Lim S, Callen E *et al.* AID expression levels determine the extent of cMyc oncogenic translocations and the incidence of B cell tumor development. *J Exp Med* 2008; **205**: 1949–1957.
12 Matsumoto Y, Marusawa H, Kinoshita K, Endo Y, Kou T, Morisawa T *et al.* Helicobacter pylori infection triggers aberrant expression of activation-induced cytidine deaminase in gastric epithelium. *Nat Med* 2007; **13**: 470–476.
13 Okazaki IM, Hiai H, Kakazu N, Yamada S, Muramatsu M, Kinoshita K *et al.* Constitutive expression of AID leads to tumorigenesis. *J Exp Med* 2003; **197**: 1173–1181.
14 Morisawa T, Marusawa H, Ueda Y, Iwai A, Okazaki IM, Honjo T *et al.* Organ-specific profiles of genetic changes in cancers caused by activation-induced cytidine deaminase expression. *Int J Cancer* 2008; **123**: 2735–2740.
15 Rucci F, Cattaneo L, Marrella V, Sacco MG, Sobacchi C, Lucchini F *et al.* Tissue-specific sensitivity to AID expression in transgenic mouse models. *Gene* 2006; **377**: 150–158.
16 Muto T, Okazaki IM, Yamada S, Tanaka Y, Kinoshita K, Muramatsu M *et al.* Negative regulation of activation-induced cytidine deaminase in B cells. *Proc Natl Acad Sci USA* 2006; **103**: 2752–2757.
17 Casellas R, Yamane A, Kovalchuk AL, Potter M. Restricting activation-induced cytidine deaminase tumorigenic activity in B lymphocytes. *Immunology* 2009; **126**: 316–328.
18 Morita S, Kojima T, Kitamura T. Plat-E: an efficient and stable system for transient packaging of retroviruses. *Gene Ther* 2000; **7**: 1063–1066.
19 Kitamura T, Koshino Y, Shibata F, Oki T, Nakajima H, Nosaka T *et al.* Retrovirus-mediated gene transfer and expression cloning: powerful tools in functional genomics. *Exp Hematol* 2003; **31**: 1007–1014.
20 Watanabe-Okochi N, Kitaura J, Ono R, Harada H, Harada Y, Komeno Y *et al.* AML1 mutations induced MDS and MDS/AML in a mouse BMT model. *Blood* 2008; **111**: 4297–4308.
21 Ye BH, Chaganti S, Chang CC, Niu H, Corradini P, Chaganti RS *et al.* Chromosomal translocations cause deregulated BCL6 expression by promoter substitution in B cell lymphoma. *EMBO J* 1995; **14**: 6209–6217.
22 Pasqualucci L, Migliazza A, Basso K, Houldsworth J, Chaganti RS, Dalla-Favera R. Mutations of the BCL6 proto-oncogene disrupt its negative autoregulation in diffuse large B-cell lymphoma. *Blood* 2003; **101**: 2914–2923.
23 Mullighan CG, Miller CB, Radtke I, Phillips LA, Dalton J, Ma J *et al.* BCR-ABL1 lymphoblastic leukaemia is characterized by the deletion of Ikaros. *Nature* 2008; **453**: 110–114.
24 Longerich S, Tanaka A, Bozek G, Nicolae D, Storb U. The very 5′ end and the constant region of Ig genes are spared from somatic mutation because AID does not access these regions. *J Exp Med* 2005; **202**: 1443–1454.
25 Aster JC, Pear WS, Blacklow SC. Notch signaling in leukemia. *Annu Rev Pathol* 2008; **3**: 587–613.
26 Mullighan CG, Goorha S, Radtke I, Miller CB, Coustan-Smith E, Dalton JD *et al.* Genome-wide analysis of genetic alterations in acute lymphoblastic leukaemia. *Nature* 2007; **446**: 758–764.
27 Ramiro AR, Jankovic M, Eisenreich T, Difilippantonio S, Chen-Kiang S, Muramatsu M *et al.* AID is required for c-myc/IgH chromosome translocations *in vivo*. *Cell* 2004; **118**: 431–438.
28 Muto T, Okazaki IM, Yamada S, Tanaka Y, Kinoshita K, Muramatsu M *et al.* Negative regulation of activation-induced cytidine deaminase in B cells. *Proc Natl Acad Sci USA* 2006; **103**: 2752–2757.
29 Liu M, Schatz DG. Balancing AID and DNA repair during somatic hypermutation. *Trends Immunol* 2009; **30**: 173–181.
30 Geisberger R, Rada C, Neuberger MS. The stability of AID and its function in class-switching are critically sensitive to the identity of its nuclear-export sequence. *Proc Natl Acad Sci USA* 2009; **106**: 6736–6741.
31 O'Neil J, Grim J, Strack P, Rao S, Tibbitts D, Winter C *et al.* FBW7 mutations in leukemic cells mediate NOTCH pathway activation and resistance to gamma-secretase inhibitors. *J Exp Med* 2007; **204**: 1813–1824.

Supplementary Information accompanies the paper on the Leukemia website (http://www.nature.com/leu)

Cytoplasmic tethering is involved in synergistic inhibition of p53 by Mdmx and Mdm2

Chihiro Ohtsubo,[1,3] Daisuke Shiokawa,[1,3,6] Masami Kodama,[1,3] Christian Gaiddon,[4] Hitoshi Nakagama,[2] Aart G. Jochemsen,[5] Yoichi Taya[1,3,6,7] and Koji Okamoto[1,2,3,7]

National Cancer Center Research Institute, [1]Radiobiology Division, [2]Early Oncogenesis Research Project, Tokyo, Japan; [3]SORST, Japan Science and Technology Corporation; [4]INSERM U692, Laboratoire de Signalisations Moleculaires et Neurode generescence, Universite de Strasbourg, Faculte de medecine, Strasbourg, France; [5]Department of Molecular and Cell Biology, Leiden University Medical Center, Leiden, The Netherlands

(Received February 17, 2009/Revised March 24, 2009/Accepted March 25, 2009/Online publication April 28, 2009)

The *mdm2* and *mdmx* oncogenes play essential yet nonredundant roles in synergistic inactivation of p53. However, the biochemical mechanism by which Mdmx synergizes with Mdm2 to inhibit p53 function remains obscure. Here we demonstrate that, using nonphosphorylatable mutants of Mdmx, the cooperative inhibition of p53 by Mdmx and Mdm2 was associated with cytoplasmic localization of p53, and with an increase of the interaction of Mdmx to p53 and Mdm2 in the cytoplasm. In addition, the Mdmx mutant cooperates with Mdm2 to induce ubiquitination of p53 at C-terminal lysine residues, and the integrity of the C-terminal lysines was partly required for the cooperative inhibition. The expression of subcellular localization mutants of Mdmx revealed that subcellular localization of Mdmx dictated p53 localization, and that cytoplasmic Mdmx tethered p53 in the cytoplasm and efficiently inhibited p53 activity. RNAi-mediated inhibition of Mdmx or introduction of the nuclear localization mutant of Mdmx reduced cytoplasmic retention of p53 in neuroblastoma cells, in which cytoplasmic sequestration of p53 is involved in its inactivation. Our data indicate that cytoplasmic tethering of p53 mediated by Mdmx contributes to p53 inactivation in some types of cancer cells. (*Cancer Sci* 2009; 100: 1291–1299)

The p53 tumor suppressor plays a central role in the prevention of tumorigenesis.[1,2] p53 exerts its function as a tumor suppressor by transcriptionally activating numerous target genes that are involved in inducing a variety of biological outcomes.[3–5] It is increasingly becoming evident that two related oncogenes, *mdm2* and *mdmx*, play central roles in the regulation of p53 activity.[6,7]

Analyses of knockout mice revealed that *mdmx* and *mdm2* suppress p53 in a nonredundant yet synergistic manner.[8] Mdmx and Mdm2 functionally cooperate to inhibit p53[9,10] and these inhibitors form a heterodimer complex through their RING finger domains.[11,12] Thus, Mdmx and Mdm2 play distinct yet cooperative functions for p53 inactivation, presumably via their physical interaction.

Mdm2 inactivates p53 by targeting it for ubiquitin-mediated proteasomal degradation and by promoting its transport from the nucleus into the cytoplasm,[13] and it is likely that inhibition of p53 by Mdm2 is attributed to these functions. Both functions of Mdm2 require the RING finger domain, which possesses E3 ubiquitin ligase activity. Indeed, Mdm2 functions as an E3 ubiquitin ligase for p53[14] although it has been reported that Mdm2 inhibits p53 via other mechanisms.[15]

In contrast to Mdm2, Mdmx lacks robust activity of an E3 ubiquitin ligase for p53[16] although Mdmx possesses a RING finger domain with high sequence similarity to that of Mdm2. In accordance with its inability to ubiquitinate p53 by itself, Mdmx-dependent inhibition of the transcriptional activity of p53 is independent of p53 degradation.[17] Recently, it was reported that Mdmx can complement the E3 activity of C-terminal mutants of Mdm2, suggesting that Mdmx contributes to p53 suppression in a manner distinct from Mdm2.[18,19]

In the present paper, by using nonphosphorylatable Mdmx mutants that are resistant to degradation by Mdm2, we showed that Mdmx and Mdm2 synergistically induce the cytoplasmic retention of p53 in DNA transfection assays. We demonstrated that cytoplasmic Mdmx, but not nuclear Mdmx, efficiently cooperates with Mdm2 to keep p53 in the cytoplasm and inhibits p53 activity. Further, RNAi-mediated inhibition of Mdmx or introduction of nuclear localization mutants of Mdmx reduced cytoplasmic retention of p53 in neuroblastoma cells. It has been documented that p53 is sequestered in the cytoplasm in some types of cancer, such as neuroblastoma, and the sequestration of p53 is likely to contribute to its inactivation. We will discuss how Mdmx and Mdm2 contribute to cytoplasmic sequestration of p53, and its implication during development of some types of cancer.

Materials and Methods

Cell lines. H1299 and U2OS cells were maintained in Dulbecco's modified Eagle's medium supplemented with 10% fetal calf serum.

Antibodies. Anti-Flag antibody (M2) was purchased from Sigma. Anti-p53 monoclonal antibody (DO-1) was purchased from Calbiochem. Anti-HA antibody was purchased from Roche (F Hoffmam-La Roche Ltd, Basel, Switzerland). Anti-myc-tag antibody (9E10), anti-GFP antibody (B-2), anti-topoisomerase I antibody (C-2), anti-γ tubulin antibody (D-10), and anti-Mdmx antibody (D-19) were purchased from Santa Cruz (Santa Cruz, CA).

DNA transfection. In DNA transfection experiments, 2 μg DNA and 4 μL Lipofectamine 2000 reagent (Invitrogen) were introduced per 2.0×10^5 cells. Transfected cells were then incubated for 20 h before harvesting. In experiments in which the subcellular localization mutants of Mdmx were transfected to determine localization of endogenous p53, Lipofectamine LTX (Invitrogen, Carlsbad, CA) was used instead according to the manufacturer's protocol.

Luciferase assay. Twenty hours after transfection, cells were lysed and luciferase activity was measured using the Dual-Luciferase Assay System (Promega, Madison, WI). Mean values (±SD) from three independent experiments were determined. Basal promoter activity expressed in the absence of HA-p53 was measured and subtracted in each experiment.

Immunostaining. Cells were fixed in 4% paraformaldehyde in PBS for 10 min, washed with 1× PBS, and permeabilized in 100% methanol for 30 min at –20°C. The fixed cells were then used for immunostaining as previously described.[20]

[6]Present address: Cancer Science Institute of Singapore, National University of Singapore, Singapore 117456.
[7]To whom correspondence should be addressed. E-mail: kojokamo@ncc.go.jp; nmiyt@nus.edu.sg

doi: 10.1111/j.1349-7006.2009.01180.x